Mon. Not. R. astr. Soc. (1992) **257**, 195–224

Stellar populations and the large-scale structure of the Small Magellanic Cloud – IV. Age distribution studies of the outer regions

L. T. Gardiner[1] and D. Hatzidimitriou[2]★†

[1]*Department of Astronomy, University of Edinburgh, Blackford Hill, Edinburgh EH9 3HJ*
[2]*Anglo-Australian Observatory, PO Box 296, Epping, NSW 2121, Australia*

Accepted 1992 January 22. Received 1992 January 16; in original form 1991 July 18

SUMMARY

The fourth in a series of papers on the large-scale structure and stellar content of the Small Magellanic Cloud (SMC), based on photometric analysis of sets of blue and red UK Schmidt photographic plates, is presented here. The previous papers reviewed the data reduction procedures and presented results on the three-dimensional structure of a large sector of the outer regions of the SMC beyond 2° from the SMC centre. Here, we present a study of the age and spatial distribution of stellar populations in an area covering six UKST survey fields, i.e. virtually the entire outer area of the SMC. The existence of a very old stellar population of age 15–16 Gyr, comprising about 7 per cent of the stellar content of the outer regions by mass, is suggested by the observational results. However, the bulk of the stellar population in the outer regions of the SMC is found to be about 10 Gyr old. The distribution of stellar populations younger than about 2 Gyr is shown to be biased towards the eastern side of the SMC facing the LMC. The star formation history of the outer regions is discussed with particular reference to the role of interactions between the LMC–SMC–Galaxy system.

Key words: galaxies: interactions – Magellanic Clouds – galaxies: photometry – galaxies: stellar content.

1 INTRODUCTION

The Magellanic Clouds are believed to have had a markedly different history of star formation from that of the Galaxy, being objects which are less evolved than the Milky Way. The SMC in particular is characterized by a low metal content, high gas-to-total mass fraction and bluer integrated colours than normal spiral galaxies (Lequeux 1984) and in these respects is typical of dwarf irregular systems. As a dwarf irregular galaxy distinguished by its membership of an interacting system of galaxies, the SMC is able to provide us with insights into the evolutionary development of dwarf irregular galaxies as well as the role of external dynamical interactions in stimulating star formation. The relative importance of star formation processes due to external disturbances and those internal to the SMC is one of the key questions yet to be properly answered.

The ultimate aim of studies of the stellar content of the outer regions of the SMC is to achieve a complete description of its star formation history from the age spectrum and spatial distribution of its stellar population. Most of our knowledge of the age distribution of the outer parts of the SMC comes from colour–magnitude diagram (CMD) studies of star clusters and adjacent regions in the SMC general field as well as from a small number of larger area studies of the SMC field population. A bibliography of deep, CCD-based studies including the reference codes we have adopted is presented in Table 1. In general, because of the small areas covered by these studies, and the fact that the observations were usually obtained with some purpose other than the detailed study of the stellar population, we do not yet have a clear idea of the distribution of various stellar populations from which to construct a coherent picture of the star formation history of the SMC.

In this paper, which is the fourth in the series on the large-scale structure and stellar content of the SMC outer regions, we aim to remedy the problem of small areal coverage and associated small-number statistics with a systematic study of the stellar population structure of the entire outer area of the

★Present address: Institute of Astronomy, Madingley Road, Cambridge CB3 0HA.
†Requests for offprints and finding charts should be addressed to D. Hatzidimitriou at the Institute of Astronomy.

Table 1. Bibliography of CMD studies of SMC clusters and field areas.

Cluster/Area	Author(s)/Year	Short Code
NGC 411	Da Costa & Mould 1986	GC1
L 113	Mould *et al.* 1984	GC2
Kron 3	Rich *et al.* 1984	GC3
L 1	Olszewski *et al.* 1987	GC4
NGC 121	Stryker *et al.* 1985	GC5
NGC 362	Bolte 1987	GC6
NGC 152	Melcher & Richtler 1989 & private communication	GC7
L 11	Buttress *et al.* 1988	GC8

SMC lying beyond 2 kpc from the optical centre. The first paper in the series (Hatzidimitriou, Hawkins & Gyldenkerne 1989 – Paper I) described part of the observational material and reduction procedures upon which the entire project is based. Two further papers (Hatzidimitriou & Hawkins 1989 – Paper II, and Gardiner & Hawkins 1991 – Paper III) presented results on the geometry of a significant fraction of the SMC outer area. The purpose of this paper is to present and discuss the stellar age distribution in an area covering virtually the entire outer area of the SMC. The observational data comprise the magnitudes, colours and positions of over a million objects on 38 photographic plates measured by the COSMOS plate measuring facility at the Royal Observatory, Edinburgh in six standard 1.2-m UK Schmidt telescope survey fields.

In Section 2 we review the observational data, a large fraction of which has formed the basis of the investigations of the large-scale structure of the SMC in Papers I–III. In Section 3, we use the properties of the main sequence to study the distribution of stellar populations as a function of their spatial position and age for fairly young stars under about 2 Gyr old. In Section 4 we investigate the older populations represented by horizontal branch stars. In Section 5 these results are discussed in relation to the overall evolutionary development of the SMC and the influence of external interactions. Section 6 states the main conclusions.

2 THE DATA BASE

2.1 The observations

The data set comprises six ESO/SERC fields (numbers 28, 29, 30, 50, 51, 52) in and around the SMC, covering a total measured area of 130 square degrees. Fig. 1 shows the overall area included in the study and the location of the various fields with respect to the main features of the SMC.

Good-quality, sky-limited, B_j (filter/emulsion combination IIIa-J/GG395) and R (IIIa-F/OG590 or IIIa-F/OG630) photographic plates taken with the 1.2-m UK Schmidt Telescope (UKST) were used. In order to improve the accuracy of the photographic photometry and to minimize the effect of position-dependent systematic errors within a

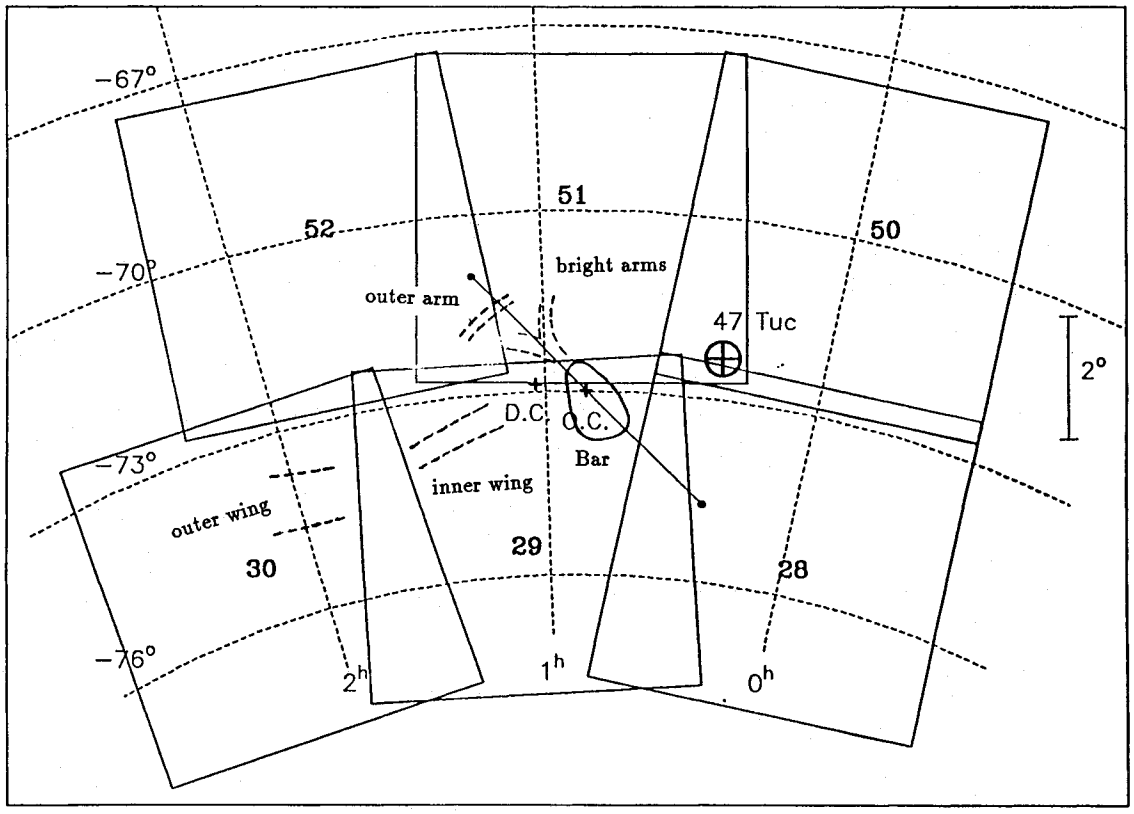

Figure 1. The locations of the ESO/SERC standard survey fields used in this study together with prominent SMC features. The optical centre (O.C.), dynamical centre (D.C.) and the SMC major axis are also marked. Equatorial coordinates are for epoch 1950.

single plate, three or four plates per filter combination and per field were used. The list of plates is given in Table 2, along with the coordinates of the centres of the fields, the dates of acquisition and the quality classification of each plate (UKST-Unit classification system).

Table 2. List of the photographic plate material used in the study together with the coordinates of the field centres. Columns 1–5 are self-explanatory. In column 6 the quality of the plates is described using the UKSTU grading system. The plates used as master-plates are followed by an asterisk.

Plate No.	Date UT	Emulsion	Filter	Exp. Time	Grade
Field 28	00^h00^m	−75°00′			
J 1935*	75-11-29	IIIaJ	GG 395	50.9	BUX2
J 3675	77-10-13	IIIaJ	GG 395	80.0	AI3
J 9553	84-08-29	IIIaJ	GG 395	70.0	aI
R 7220	81-09-28	IIIaF	RG 630	100.0	CIU6
R 9587*	84-09-20	IIIaF	RG 630	90.0	aH
R 9600	84-09-23	IIIaF	RG 630	95.0	a
Field 29	01^h06^m	−75°00′			
J 1940	75-11-30	IIIaJ	GG 395	60.0	BIS2
J 1948*	75-12-03	IIIaJ	GG 395	60.0	A2
OR11406*	86-10-01	IIIaF	OG 590	45.0	BEI3
OR13439	89-11-21	IIIaF	OG 590	65.0	A3
OR13908	90-10-11	IIIaF	OG 590	75.0	a
Field 30	02^h12^m	−75°00′			
J 1805	75-09-08	IIIaJ	GG 395	60.0	BE2
J 8844*	83-10-08	IIIaJ	GG 395	60.0	A2
J13917	90-10-13	IIIaJ	GG 395	80.0	a
OR13260*	89-08-29	IIIaF	OG 590	75.0	BI3
OR13500	89-12-18	IIIaF	OG 590	60.0	BIE4
OR13834	90-09-16	IIIaF	OG 590	60.0	aI
Field 50	00^h00^m	−70°00′			
J 905	74-09-11	IIIaJ	GG 395	40.0	B
J 3670*	77-10-12	IIIaJ	GG 395	75.0	A2
J12700	88-08-11	IIIaJ	GG 395	85.0	BEI4
J12720	88-08-19	IIIaJ	GG 395	100.0	CIU5
OR10385	85-08-17	IIIaF	OG 590	75.0	BUIE4
OR11282	86-08-10	IIIaF	OG 590	70.0	BID3
OR12192*	87-09-24	IIIaF	OG 590	85.0	AUE3
OR12728	88-08-20	IIIaF	OG 590	95.0	AI3
Field 51	00^h52^m	−70°00′			
J 1800	75-09-07	IIIaJ	GG 395	60.0	BIE3
J 1829	75-10-03	IIIaJ	GG 395	70.0	BI3
J 1877*	75-10-31	IIIaJ	GG 395	70.0	A1
J13369	89-10-05	IIIaJ	GG 395	60.0	BI4
OR10440*	85-09-08	IIIaF	OG 590	75.0	BI4
OR12821	88-10-30	IIIaF	OG 590	95.0	BI4
OR13318	89-09-24	IIIaF	OG 590	75.0	AEI3
Field 52	01^h44^m	−70°00′			
J 1825	75-10-02	IIIaJ	GG 395	70.0	AIF3
J 2566*	76-09-01	IIIaJ	GG 395	60.0	AI2
J 3671	77-10-12	IIIaJ	GG 395	75.0	BE2
R10516	85-10-17	IIIaF	RG 630	95.0	a
R10640*	86-01-02	IIIaF	RG 630	115.0	aT
OR12169	87-09-20	IIIaF	OG 590	90.0	BEI4

Grading system. E: emulsion fault; F: fogging; I: image size > 35 μm; U: underexposed; UX: although underexposed, no obvious difference from the survey plate; H: haze haloes (affecting only the brightest stars); T: trail. A, B and C refer to survey-quality grades (A being the best quality plate); a, b, c refer to non-survey-quality grades.

The photographic plates were digitized using the high-speed microdensitometer COSMOS at the Royal Observatory, Edinburgh (see e.g. MacGillivray & Stobie 1984). The procedures used to process the COSMOS data, to combine the various plate measurements and to derive the instrumental magnitudes and their transformation to the standard Johnson/Cousins photometric system are described in detail in Papers I and III. The calibration of the photographic magnitudes was achieved using a series of CCD photometric sequences established at different observatories, namely the European Southern Observatory using the 1.5-m Danish telescope in 1987 and 1988, and Siding Spring Observatory in 1987 using the 3.9-m Anglo–Australian Telescope (during service time). The photometric sequences for Fields 28 and 52 can be found in Paper I, those for Fields 50 and 51 in Paper III and finally those for Fields 29 and 30 can be found in Appendix A. (Identification charts for sequences in Fields 29, 30, 50 and 51 are also available on request from DH.)

An extensive analysis of the possible sources of error in the photographic photometry can be found in Papers I and III. The random photometric errors are estimated to be in the range 0.06–0.10 mag. Position-dependent systematic errors in the photometry are also present, caused by a variety of factors such as changes of image structure across a plate, geometrical vignetting and sensitivity variations in the emulsion of a plate. By combining 3–4 plates per field and per filter such systematic errors peculiar to individual plates can be minimized. However, there remain large-scale variations common to all plates of which vignetting at the edges of plates is probably the most significant. These remaining effects can be monitored by comparing the photometry in the overlapping regions of neighbouring fields. Photometric comparisons were performed between Fields 52–51, 50–51, 50–28 and 30–29. Fig. 2 shows the magnitude differences for paired stars in the aforementioned field overlaps for the B_j and R filters. In general, the *mean* differences between the photometry in overlapping fields are less than 0.2 mag. In the following we take account of possible systematic errors of the order of 0.2 mag in the derived colours and magnitudes of stars in different fields, but it must be emphasized that the reported errors are upper limits for the errors in the central parts of the plates, due to larger systematic errors at the plate edges.

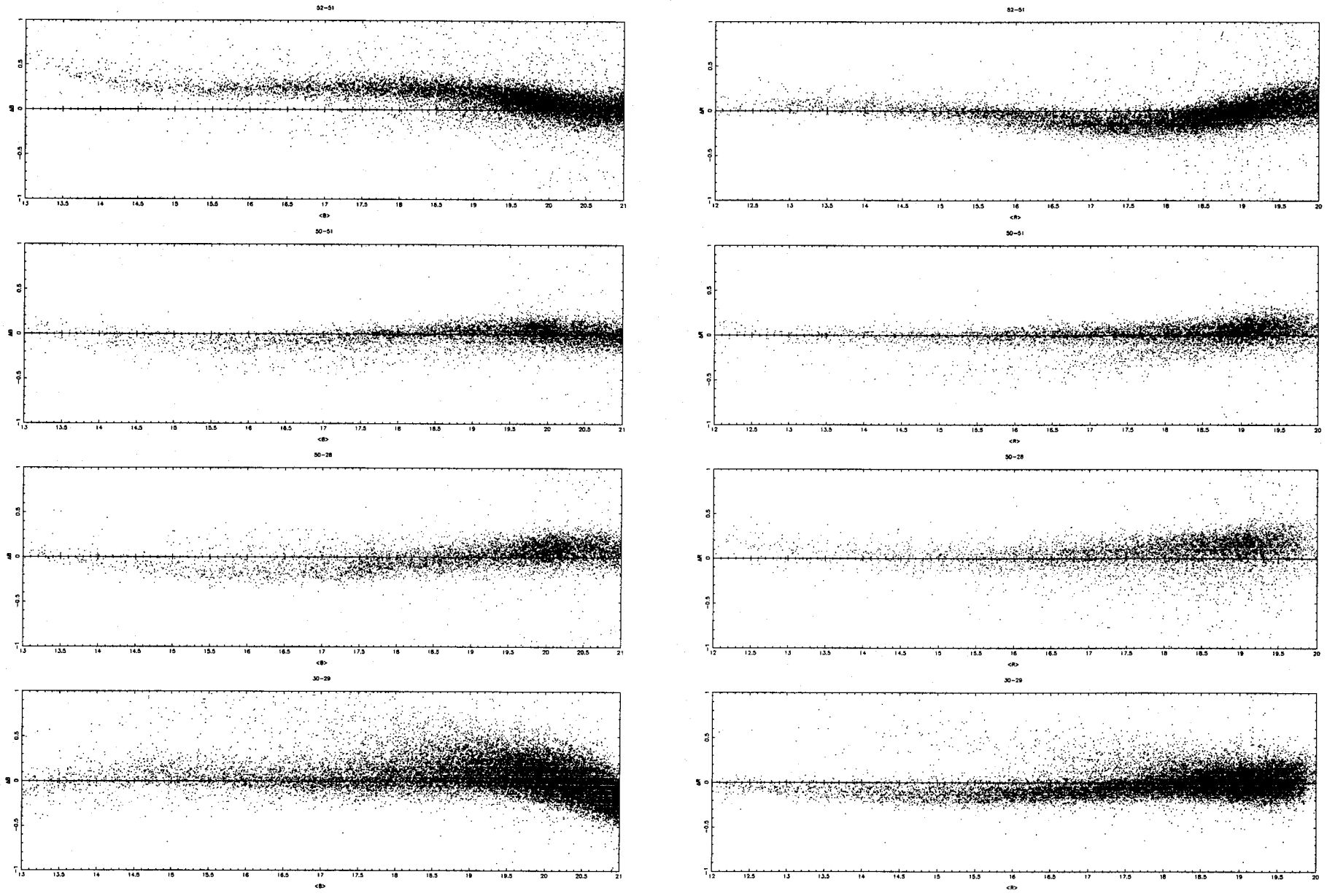

Figure 2. Photometric comparisons in the overlap areas between the fields. The differences between photometry of individual images from different fields for the overlapping fields 52–51, 50–51, 50–28 and 30–29 are shown for the B_J and R wavebands. The axes are as follows. Left-hand panels: ΔB (-1 to 1) against $\langle B \rangle$ (13 to 21). Right-hand panels: ΔR (-1 to 1) against $\langle R \rangle$ (12 to 20).

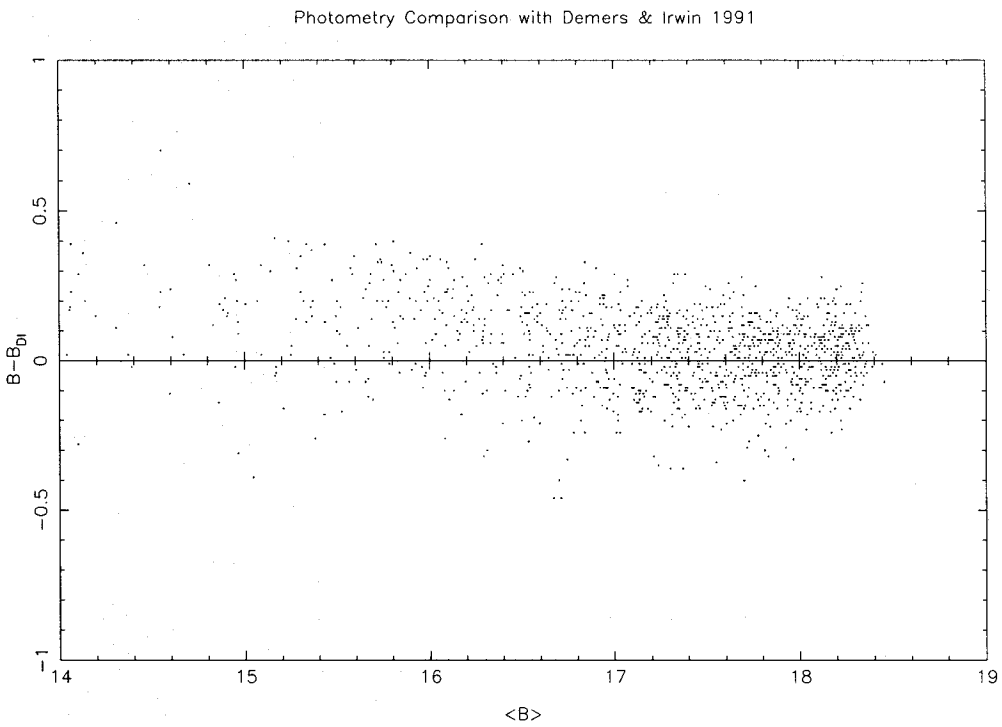

Figure 3. Comparison between the photometry of blue stars in Field 30 with that of Demers & Irwin (1991). For 1217 stars common to the two magnitude lists, the differences between the B magnitudes have been plotted against the mean B magnitude.

The B-band photometry for Field 30 was also compared with the published photographic photometry by Demers & Irwin (1991) of blue stars in the Wing/inter-Cloud region (see Fig. 3). The agreement is very good for stars fainter than $B \sim 16.5$ mag. The zero-point difference between the two sets of independently derived magnitudes did not exceed 0.10 mag and the 1σ dispersion in the magnitude difference was found to be 0.13 mag, which is comparable to the size of the random errors estimated above.

Paper I discussed the completeness of the data base, and concluded that the areas included in the study are about 95 per cent complete except for the faintest images. We have conducted further studies of the completeness which indicate that crowding resulting in multiple images can be a problem for areas with image densities in excess of 4 images per arcmin^2. Most of these multiple images are unmatched due to measurements from different plates giving variable parameters for the images, in some cases resolving the multiple images. The numbers of images lost in this way do not depend significantly on the magnitude; Penny & Dickens (1986) confirm that loss of images in crowded fields is evenly distributed with respect to magnitude. However, for very close pairs of stars, which tend to be matched on all the plates, there is a magnitude dependence of the percentage of images lost. This is because, first, a faint image close to a bright one will make the bright one brighter while the faint one will not be detected and, secondly, two close faint images may result in an apparent single image with a brighter magnitude. Inspection of photographic prints of sample areas of UKST plates indicates that, even for the most crowded areas within 2° of the SMC centre, less than 20 per cent of the stars in the final data set are closely merged multiple images. Therefore we conclude that the differential loss of faint images with respect to bright images is not very significant. The overall incompleteness is affected more by pairs or groups of stars being lost altogether due to their not being matched on one or several plates. About 10–15 per cent of such images are lost for areas with image densities above 4 images per arcmin^2, rising to about 30 per cent for areas with 10 images per arcmin^2. The areas within 2°.5 of the SMC centre in Fields 51 and 52, together with the areas within 3° of the SMC centre in Fields 28 and 29, have image densities in excess of 4 images per arcmin^2 and are thus affected by the incompleteness of greater than 10 per cent described here. However, as we will see later, the continuity in the surface counts of different stellar populations (Figs 5 and 8) shows that the level of incompleteness is uniform from field to field. Areas with very high number densities (above 10 images per arcmin^2) were not included in this study; such areas include the central regions of the SMC, and regions near the galactic globular clusters 47 Tuc and NGC 362 which are not of interest here.

Another aspect of the incompleteness is the random loss of faint images due to the lower signal-to-noise ratio near the detection limit. Fig. 4 shows, as a function of magnitude for a sample field (Field 51), the percentage of images matched on all three plates with respect to the total number of images on the single plate used as the 'master' plate in the matching procedure. In all cases, the deepest plate with the largest total number of images was selected as the 'master' plate. The plot shows that there is significant incompleteness (about 20 per cent unmatched images) at about 0.5 mag above the effective magnitude limit set by the combination of the true plate limit and the limit applied by the COSMOS software. This limit is different for different fields, with incompleteness for some fields at magnitudes as bright as $R = 19.5$.

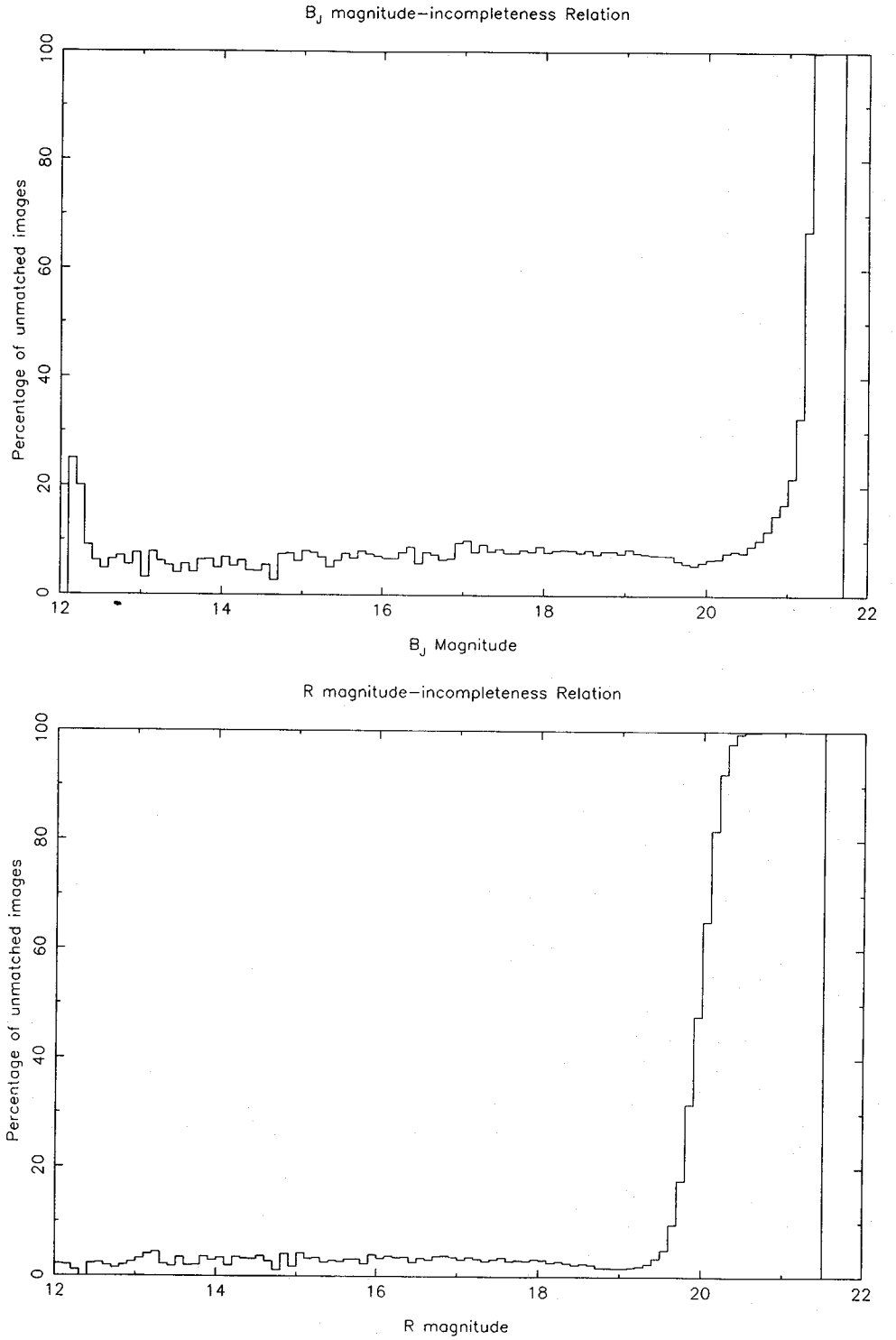

Figure 4. Incompleteness in the photographic photometry. The percentage of unpaired images (i.e. images not matched up on other plates in the same field) with respect to the total number of images on the master plate in Field 51 as a function of magnitude for B_J and R wavebands is shown.

2.2 The colour–magnitude diagrams

After application of the calibration processes described above, positional, colour and magnitude data for a total of 1.1 million images comprised the data base for the study of the stellar populations in the SMC outer parts. Each field was divided up into 'grid' regions, each being a square of $0.^{\circ}93 \times 0.^{\circ}93$. A colour–magnitude diagram in R versus $B-R$ was then constructed in each of these grid regions. In this way, the positional dependence of the relative contributions of the populations in the SMC field could be studied. In Appendix B, we present representative examples of CMDs

in each of the ESO/SERC fields studied. The various features observed in the CMDs are a well-defined red giant branch, a densely populated red horizontal branch or clump, a subgiant branch, and a main sequence comprising relatively young stars (see fig. 4 of Paper III for identification of these features).

Two further methods were employed to study the positional variation of the properties of different stellar populations. The first involves the production of contour maps in order to gain an overview of the population distribution. The technique and results are described in the following section. The second involves the use of circular grids for each field centred on the SMC optical centre at RA=00^h51^m, Dec.=$-73°$, 1950 (de Vaucouleurs & Freeman 1972). This method ensures more uniform statistics at different distances from the centre, but it presumes radial symmetry and smears out any localized features. Nevertheless, in some cases, and after the overall distribution was studied, circular grids were used (see Section 3) for statistical reasons.

3 THE MAIN SEQUENCE

The main-sequence (MS) chronology is one of the main tools for investigating the ages of stellar populations in star clusters and field populations. In this section, we first discuss the use of an age calibration scheme to date the MS populations in the outer regions of the SMC (Section 3.1); secondly, we present the overall surface distribution of MS populations detected above our effective magnitude limit at $R=20$ (Section 3.2), and finally we analyse the main-sequence luminosity functions and present age distribution plots for the areas studied (Section 3.3).

3.1 The age-dating of main-sequence populations

The age-dating procedure involves the comparison of theoretical isochrones with the observed colour–magnitude diagram of the stellar population. From consideration of the luminosity functions associated with such isochrones, Da Costa, Mould & Crawford (1985) suggested that the best feature from which to date clusters (or coeval populations) in the age range of a few Gyr is the 'tip' of the MS, i.e. the point on the isochrone where rapid evolution to the red begins. The age calibration which we will employ is the revised calibration of Hodge (1987a), based on observational data for a large number of Magellanic Cloud clusters in conjunction with the theoretical isochrones of VandenBerg (1985). The relation between the B magnitude of the MS 'tip' and the age of the stellar population at the small distance modulus of the SMC ($dm=18.8$) is given by the equation

$$\log_{10}(\tau/\mathrm{yr}) = 2.58 \pm 0.335\ B.$$

Inspection of the CMDs in Appendix B shows that the MS locus has a roughly constant colour of $B-R=-0.1$ above the effective magnitude limit, so the relation for the R magnitude of the MS 'tip' becomes

$$\log_{10}(\tau/\mathrm{yr}) = 2.55 + 0.335\ R. \qquad (1)$$

According to equation (1) the age of the oldest MS population that can be detected above our effective magnitude limit at $R=20$ is 1.8 Gyr. The metallicity range in the SMC ([Fe/H]=-1.4 to -0.7 dex; e.g. Da Costa 1991) does not have a significant effect (compared to the other factors described below) on the estimated value of the 'tip', especially for populations younger than 1–2 Gyr which are likely to be more metal-rich than -1.0 dex.

The main factor which may affect this age calibration is uncertainty in the distance of the stellar populations in the SMC. Hodge's calibration has made use of the small distance modulus scale for the Magellanic Clouds which has come to be favoured recently (see Paper II). A problem related to the uncertainty in the distance modulus of the SMC is the question of the extension of the SMC along the line-of-sight direction. As discussed by Martin, Maurice & Lequeux (1989), there is debate concerning the depth of the SMC, with claims for a depth not exceeding the tidal diameter (about 8 kpc) (Welch *et al.* 1987) competing with estimates of 20–30 kpc by other authors (Caldwell & Coulson 1986; Mathewson, Ford & Visvanathan 1986). These determinations refer mainly to the central regions of the SMC excluded from this present study. However, for the outer regions, results from Papers II and III provide strong evidence (from the luminosity distribution of clump stars) for large depths along the line-of-sight direction of at least 20 kpc in the north-east (NE) outlying area. The mean distance moduli determined for the grid regions in the NE area are smaller than corresponding determinations for the west (W) and south-west (SW) areas (Papers II, III), and fig. 11 in Paper III shows that the front section of the NE area extends to distance moduli as low as 18.4, i.e. 0.4 mag less than the small distance modulus (18.8) of the SMC main body. This distance information is used in the present work to provide corrections to the age calibration of equation (1) where necessary, but it must be emphasized that large depths along the line of sight may lead to some ambiguity in the interpretation of the MS luminosity functions. For MS populations with a distance modulus of 18.4, the corresponding ages are about 33 per cent higher than those given by equation (1) for a given apparent magnitude.

Another factor which may affect the age calibration is differential reddening in the SMC. Hodge's calibration incorporates the effects of reddening towards the SMC, which is generally considered to be small. The value derived for the outer regions of the SMC in Paper I was $A_R=0.07$ mag. Higher reddening values may exist, however, for the central regions and the Wing region where the H I surface density is much greater. Caldwell & Coulson (1985, 1986) obtained *BVI* reddenings of Cepheids located in the inner SMC regions and in the Wing, and determined a mean colour excess of $E(B-V)=0.054$, corresponding to $A_R=0.13$. Since the reddening is not much greater in these areas compared to the outlying areas, and in any case we are dealing mainly with regions outside the area of the Cepheid study, there is little advantage to be gained in incorporating a correction for differential reddening, given the level of precision of both the photometric data and the age calibration.

3.2 The surface distribution of main-sequence stars

Blue main-sequence stars visible above the plate limit provide us with the possibility of mapping the surface distribution of stars younger than about 2 Gyr, according to the above discussion on the ages of stellar populations corre-

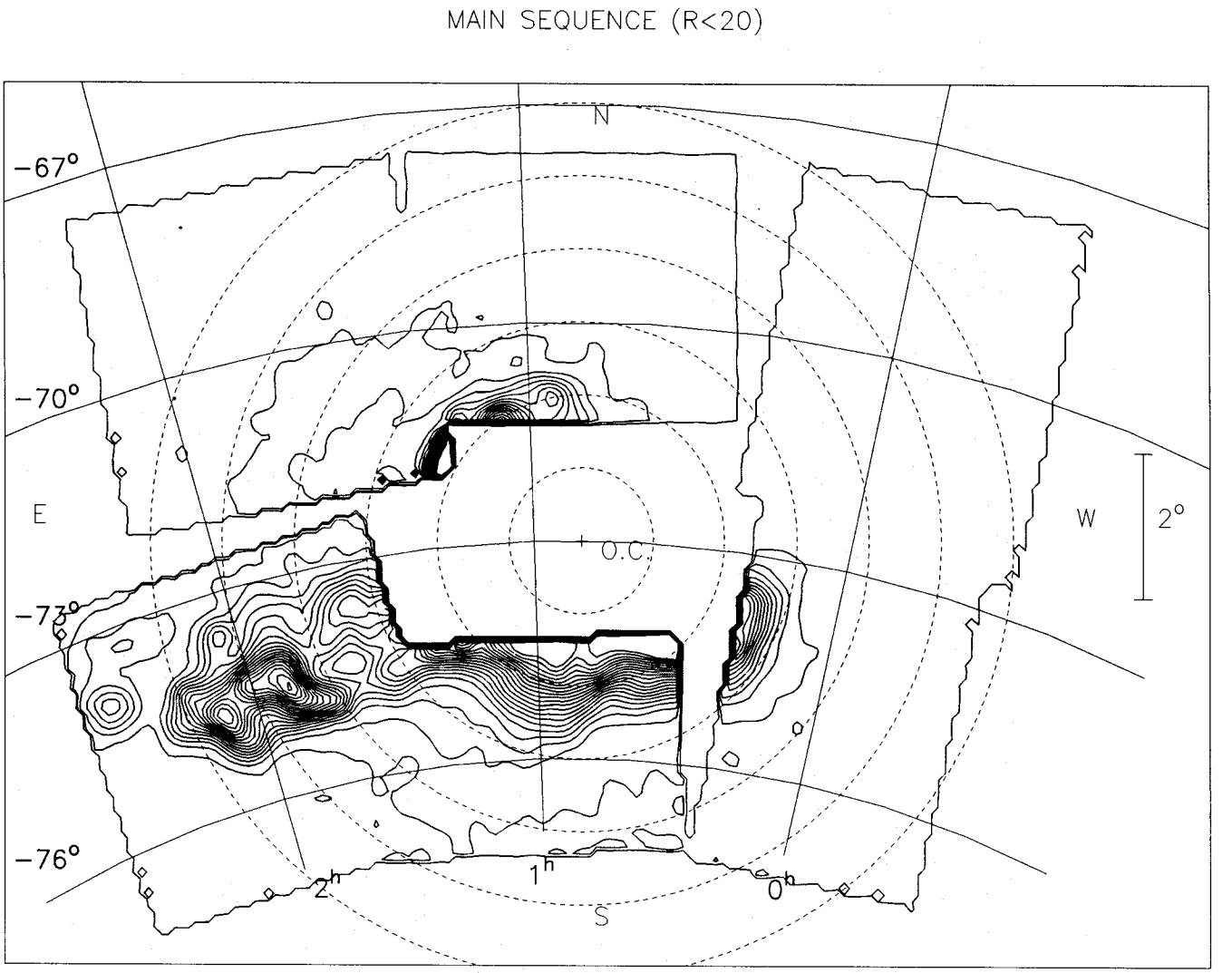

Figure 5. Contour plot of the surface distribution of main-sequence stars with $B-R<0.1$, $R<20$ for all six survey fields. Concentric radii at 1°, 2°, 3°, 4°, 5°, 6° from the SMC optical centre are shown. The contour levels generally increase towards the SMC centre and consist of levels of 1, 3, 5, 7 stars per pixel. To obtain the number of stars per square degree, multiply by 115.

sponding to various MS 'tip' luminosities. Using the full data base from all six survey fields we selected MS populations on the basis of their locations in colour–magnitude space with limits of $R<20$, $B-R<0.1$. Number counts for the MS population were performed using pixels of size 5 mm square (5.6 arcmin square) and subsequently smoothed with a Gaussian filter with $\sigma=9.7$ arcmin. The pixel array was then contoured, and the isodensity plot for the MS population is shown in Fig. 5. There is essentially no contribution from the galactic foreground to the MS counts, as the MS stars lie blueward of the 'yellow ridge' due to spheroidal component subgiants in the Galaxy.

We move now to a brief discussion of the main features of the MS distribution corresponding to the distribution of stars younger than about 2 Gyr. The complete absence of MS stars above the detection limit in the north-west is striking, while there is a considerable MS population over a large part of the eastern and southern area. Very prominent in the east is the SMC Wing feature, which is known to consist of extreme Population I objects such as blue and yellow supergiants, OB associations and H II regions (Westerlund 1970). Also conspicuous is a 'bulge' in the surface distribution in the SSE direction. Along the NE–SW line on either side of the optical centre there appear to be MS populations comprising extensions of the SMC main bar. These areas are characterized by steeply rising numbers with decreasing distance from the optical centre as shown by the very closely spaced contours. The MS contour plot gives us an overview of the distribution of a younger (less than 1.8–2.4 Gyr depending on the distance modulus) subset of the total stellar population, but in order to obtain a more refined picture of the age distribution of these younger populations we have to perform an analysis of the MS luminosity functions, which is the purpose of the next subsection.

3.3 Main-sequence luminosity functions

With the aid of the contour plot for the MS distribution as a guide to likely changes in the population structure, we have constructed MS luminosity functions (LF) for stars lying

Table 3. Data for the circular grid regions used for the main-sequence LF study. Column 1 gives the region name (including the Field no.), column 2 gives the inner and outer distances from the SMC centre in degrees enclosing each region, column 3 gives the logarithmic offset added to log (number counts per bin) for the LF plots in Fig. 6, and column 4 gives the symbols used in Fig. 6 to denote the LF for each region.

Region	Inner/Outer Radii (deg.)	Plot Offset	Plot Symbol
Wing (IDK)	–	0.3	Filled square
F30 (Inner)	3/4	0.3	Triangle
F30 (Middle)	4/5	0.1	Circle
F30 (Outer)	5/8	0.0	Curve
F29 Centre (Inner)	2/2.5	0.0	Filled square
F29 Centre (Outer)	2.5/4	0.3	Triangle
F29 West	2.3/3	0.0	Filled square
F52 (Inner)	2/2.5	0.0	Filled square
F52 (Outer)	2.5/4	0.0	Triangle
F51 (Inner)	2/2.5	0.0	Filled square
F51 (Outer)	2.5/3	0.7	Triangle
F28	2/3	0.0	Filled Square

between circular annuli centred on the SMC optical centre. We have used bins of size 0.5 mag from $R=13$ to 20 to obtain the number of stars per bin, N, and then calculate the logarithmic luminosity function, $\log N(R)$, which allows a simple shift along the y-axis when intercomparing various LFs. The faintest magnitude bin, $R=19.5$–20.0, suffers from incompleteness due to proximity to the plate limit, so will largely be ignored in the following analysis. Table 3 lists the regions for which the LFs have been constructed, the radial limits within which the stars lie for each region (referred to the optical centre), the logarithmic offset added to the actual $\log N$ statistics to give $\log \phi$ (the scaled luminosity function) in the plots of the various LFs shown in Fig. 6, and the symbol used for the LF data in these plots. For Field 29, we have derived two sets of LFs, one for the central section and one for the western section. From the shape of the MS contours there appears to be a 'bulge' in the MS distribution in a SSE direction. The LF of the central section represents this 'bulge', while the other LF is due to the western part of Field 29 away from the 'bulge'. The extreme eastern part of Field 29 contains a contribution from the SMC Wing and has not been plotted.

The interpretation of the LF of a superposition of populations of different ages is a non-trivial task, since identification of distinct age components is hampered by reduced contrast in the turn-off area. We can, however, make some progress using a technique involving the comparison of the LF slopes with some 'initial LF', on the assumption that this initial LF has remained constant within the SMC over the past 2 Gyr. We have to hand the LF of the SMC Wing region which we shall show is due to an essentially coeval stellar population whose slope represents an initial LF over the range $-5<M_R<1$. In what follows we analyse the luminosity functions of Fig. 6 with the aid of the approximate turn-off luminosities for different ages given by equation (1), taking into account the effect of the large depth of some areas of the SMC.

3.3.1 *The SMC Wing region (Field 30)*

We consider first the MS luminosity functions of the SMC Wing in order to explore the possibility that the stellar populations of the Wing can provide us with a general 'initial luminosity function' for a coeval stellar population in the SMC. The work of Irwin, Demers & Kunkel (1990) on the outer Wing of the SMC and the inter-Cloud region showed that the composite LF for several blue stellar aggregates in the outer Wing (east of RA$=2^h15^m$, Dec.$=-74°$) was virtually identical to the LF determined for several Magellanic Cloud clusters by Mateo (1988). The area covered by the study by Irwin *et al.* overlaps the easternmost area of Field 30, so it is not surprising that our LFs for the Wing region are similar to theirs. In Fig. 6 (Field 30 Wing) their LF is shown together with three other LFs representing the inner, middle and outer areas in Field 30. Agreement between the four LFs is very good for $R<18$, whereas fainter than this the LFs of the inner and middle areas are slightly steeper than that of the outer area. This is almost certainly due to the presence of an older stellar population superimposed on the inner part of the Wing. The difference in $\log \phi$ is about 0.1, indicating that this population comprises about one-fifth of the numbers of MS stars in this section of the LF. Thus only the LF for the outer area can be considered to be the true Wing LF. From visual inspection of CMDs in Field 30 (see Appendix B) it appears that the brightest MS stars reach $R=15.5$, making the age of the SMC Wing about 50×10^6 yr according to equation (1).

The resemblance of the Wing LF to the LF of the Magellanic clusters observed by Mateo (1988), noted by Irwin *et al.*, not only supports the existence of a global initial mass function for the Magellanic Clouds but also confirms that the SMC Wing was created by a single star formation event. Mateo's study included clusters up to 2.5 Gyr in age, so we are justified in using the assumption that the LF of the SMC Wing region represents a uniform 'initial LF' for the SMC over the past ~2 Gyr to infer the age distribution in other parts of the SMC outer area. To do this correctly we also need to know whether the distance modulus for the SMC Wing differs from the small distance modulus of the SMC. The study of SMC structure using Cepheids by Caldwell & Coulson (1986) (see their fig. 7) showed that Cepheids in the Wing (the 'near arm') have a distance modulus 0.3 mag less (nearly 8 kpc) than that of the centroid of the main bar. Therefore, we have to shift the LF of the Wing by 0.3 mag (fainter) in order to derive the 'initial LF' applicable to our adopted distance modulus. In the LF plots in Fig. 6 the luminosity-shifted LF of the outer Wing region (the 'initial LF') has been superposed on the LF of the other regions.

3.3.2 *The remaining outer areas*

Examination of the plots of the luminosity functions in Fig. 6 reveals that, for the inner studied areas lying within 2°.5 of the SMC centre plus the LFs for Fields 28 and 29 (west), for which most of the MS stars lie within 3° of the SMC centre, the slopes of the logarithmic luminosity functions are shallower than those for the outlying regions for the section fainter than $R=18$. The inner areas have higher image densities than the outer areas, so one may ask whether the turnover in the LFs in the inner areas is due to

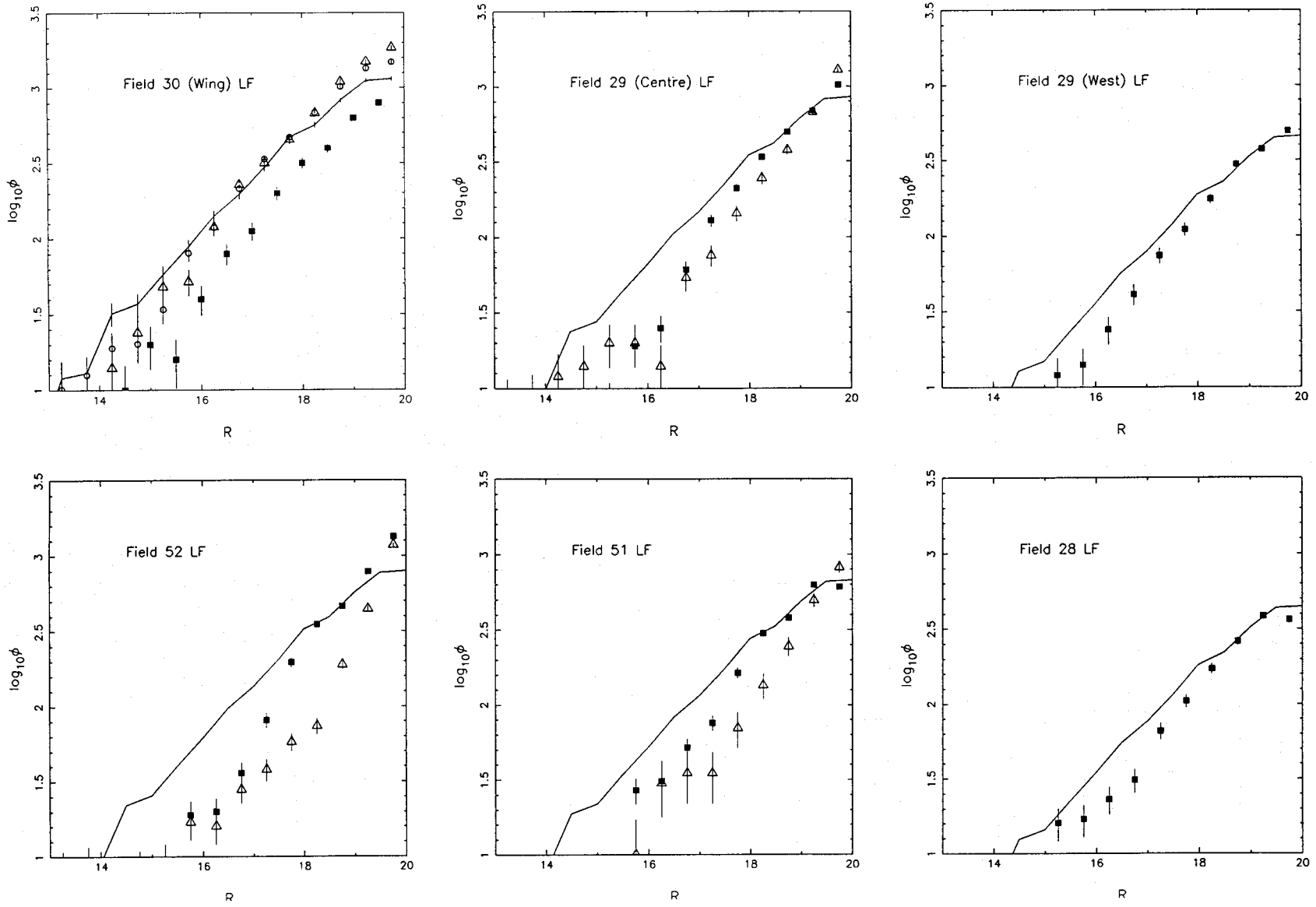

Figure 6. Main-sequence differential luminosity functions for several circular grid regions compared with a superposed luminosity function from the Wing region representing an 'initial luminosity function'. The faintest magnitude bin, 19.5–20.0 mag, suffers from significant incompleteness as can be seen from the turnover in the number counts in some luminosity functions. Symbols: *Field 30* – triangle – inner, circle – middle, curve – outer regions. The filled-square symbol denotes the luminosity function obtained by Irwin, Demers & Kunkel (1990); *Field 29 Centre* – filled square – inner, triangle – outer regions; *Field 29 West* – filled square; *Field 52* – filled square – inner, triangle – outer regions; *Field 51* – filled square – inner, triangle – outer regions; *Field 28* – filled square. See Table 3 for precise definitions of these regions.

incompleteness affecting magnitudes. As discussed fully in Section 1, the incompleteness in the data set, although increasing towards the more crowded inner regions, is largely independent of magnitude. In any case, an excess incompleteness of over 100 per cent at $R=19$ compared to that at $R=18$ is required to make the slope of the LF of the inner region in Field 52 identical to that of the outer region, so the differences in the shapes of the LFs for this field do appear to demonstrate a true difference in the age composition of the inner and outer areas.

The inner areas of the northern Fields 51 and 52 both have a fairly well-defined break in their LFs at $R=18$, after which the LF follows the initial LF quite closely. We can thus infer the presence of a population component aged about 0.4–0.6 Gyr, depending on the distance modulus applicable to the MS populations. The uncertainty in this age determination is due to the uncertainty in the distance modulus, which is in the range $dm=18.4$–18.9, since these areas possess larger line-of-sight depths than most other areas (see Papers II and III). In the western and southern inner areas, [Fields 28 and 29 (west)], a strong break in the LFs is not seen, but the slopes of the LFs follow the shape of the initial LF in the section fainter than $R=18.5$. This indicates the existence of a component of similar age to the inner areas in Fields 51 and 52, about 0.6 Gyr, but younger populations up to 0.2 Gyr old (MS 'tip' luminosity, $R=17.2$) are also present in significant numbers.

The LFs for the outlying areas in Fields 51, 52, and 29 (central 'bulge' region) all have fairly steep slopes exceeding the initial LF slope along all sections of the LF. This can be ascribed to the presence of a series of MS 'turn-offs' along the LF, with the increasing deficit in star numbers with respect to the superposed initial LF with decreasing magnitudes indicating that the contribution of younger populations is declining with decreasing age. Therefore, for populations aged up to about 1.2 Gyr, which is the limit defined by the completeness limit at $R=19.5$, the age spectrum is to a greater extent biased towards older ages in the outer area and it can be concluded that the younger (0.4–0.6 Gyr in age) populations fade rapidly in these outer regions with increasing distance from the SMC centre. Since these outer areas generally coincide with areas possessing large line-of-sight depths, the LFs could have been made steeper by the effect of older populations being 'brought up' in luminosity.

3.3.3 *Age distribution contour maps*

As an aid to visualizing the surface distribution of stellar populations of different ages, we have constructed contour plots which show the relative contribution from various age ranges to the total stellar population aged less than 1.2 Gyr (for simplicity we have assumed that all stars lie at the same distance modulus). We have split up the MS stars into three groups on the basis of their R magnitudes; the first group defined by $16.5<R<17.5$ comprises stars including all ages younger than 0.3 Gyr (we call this the 'very young' group), the second group defined by $17.5<R<18.5$ comprises stars younger than 0.6 Gyr (we call this the 'young' group), and the third group defined by $18.5<R<19.5$ comprises stars younger than 1.2 Gyr (we call this the 'older' group). We have constructed two surface distribution plots by processing data in a similar way to that described above for the overall distribution of MS stars. The first plot shows the relative contribution of stars younger than 0.3 Gyr to the total population aged up to 1.2 Gyr and has been constructed by dividing the numbers of stars (on a pixel-by-pixel basis) in the 'very young' group by the number of stars in the 'older' group and using a scaling factor to take account of the shape of the initial LF. This scaling factor has been calculated so that areas with a luminosity function identical to our initial LF (i.e. the Wing region) have a ratio of unity, i.e. the 'very young' population makes up 100 per cent of the total stellar population. The second plot shows the relative contribution of stars younger than 0.6 Gyr to the total population aged up to 1.2 Gyr. The plots are shown in Fig. 7, with three contour levels – 0, 50 and 90 per cent, indicated by white-, grey- and dark-shaded areas respectively.

There is much noise in the plots due to poor statistics in the outermost areas populated by MS stars. Nevertheless, these contour maps essentially reinforce the findings of the LF analysis above, showing that younger populations (<0.6 Gyr in age) are concentrated towards the centre of the SMC and in the Wing region. Other areas populated by MS stars display an older age constitution, notably the NE outer area which has low numbers of 'young' and 'very young' stars and part of the S and SW areas which have small numbers of 'very young' stars.

The appearance of these contour maps in the Wing region (Field 30) can tell us also about the distribution of MS populations other than those directly associated with the Wing feature but which happen to lie on the same line of sight. These maps show a fall-off in the contribution of younger populations in the northernmost and westernmost parts of Field 30 (the Wing area). We noted earlier that a contribution from an older underlying population has affected the LFs for the inner part of the Wing. Since this older population is more centrally concentrated than the younger 'Wing' population, this is reflected in the proportionally reduced contribution of 'very young' and 'young' stars within 4° of the SMC centre.

4 THE CLUMP/HORIZONTAL BRANCH AND THE OLDER POPULATIONS

The clump/red-horizontal-branch (red HB) is the most conspicuous feature of the CMD in the SMC general field studied here, with the exception of the Wing region (Field 30), where young stars populating the MS dominate (Section 3). Stellar populations belonging to a wide range of ages display purely red horizontal branches, the youngest being a few 10^8 yr old such as open clusters in our own Galaxy, while the oldest can be as old as the galactic globular clusters 47 Tuc, Palomar 4 and Eridanus, i.e. around 15 Gyr old. The 'clump' describes the red HB of younger populations, while a more 'horizontal' structure seems to be appropriate for older populations.

In this section we first present the overall surface distribution of the clump/HB stars (Section 4.1); secondly, we analyse the structure of the observed HB to derive information about the major age contributors in the SMC general field (Section 4.2); finally, in Section 4.3 we investigate the oldest populations in relation to the structure of the HB and discuss the absence of a blue HB in our CMDs.

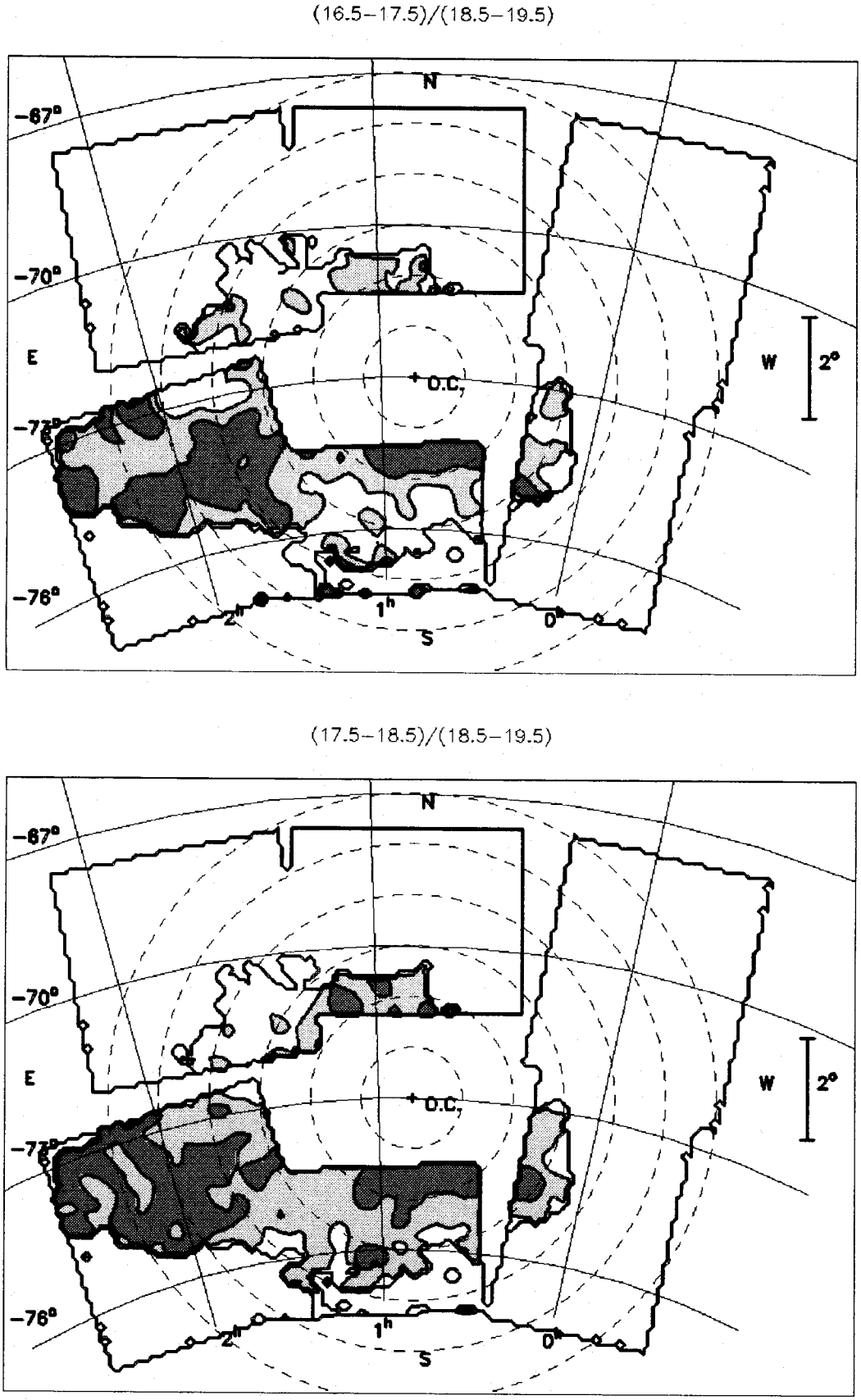

Figure 7. Age distribution contour maps. The top diagram shows the relative contribution of 'very young' (< 0.3 Gyr) main-sequence populations defined by $16.5 < R < 17.5$ to the total population younger than about 1.2 Gyr. The bottom diagram shows the relative contribution of 'young' (< 0.6 Gyr) main-sequence populations defined by $17.5 < R < 18.5$ to the total population younger than about 1.2 Gyr. On both plots three contour levels are shown – 0, 50 and 90 per cent, indicated by white-, grey- and dark-shaded areas respectively.

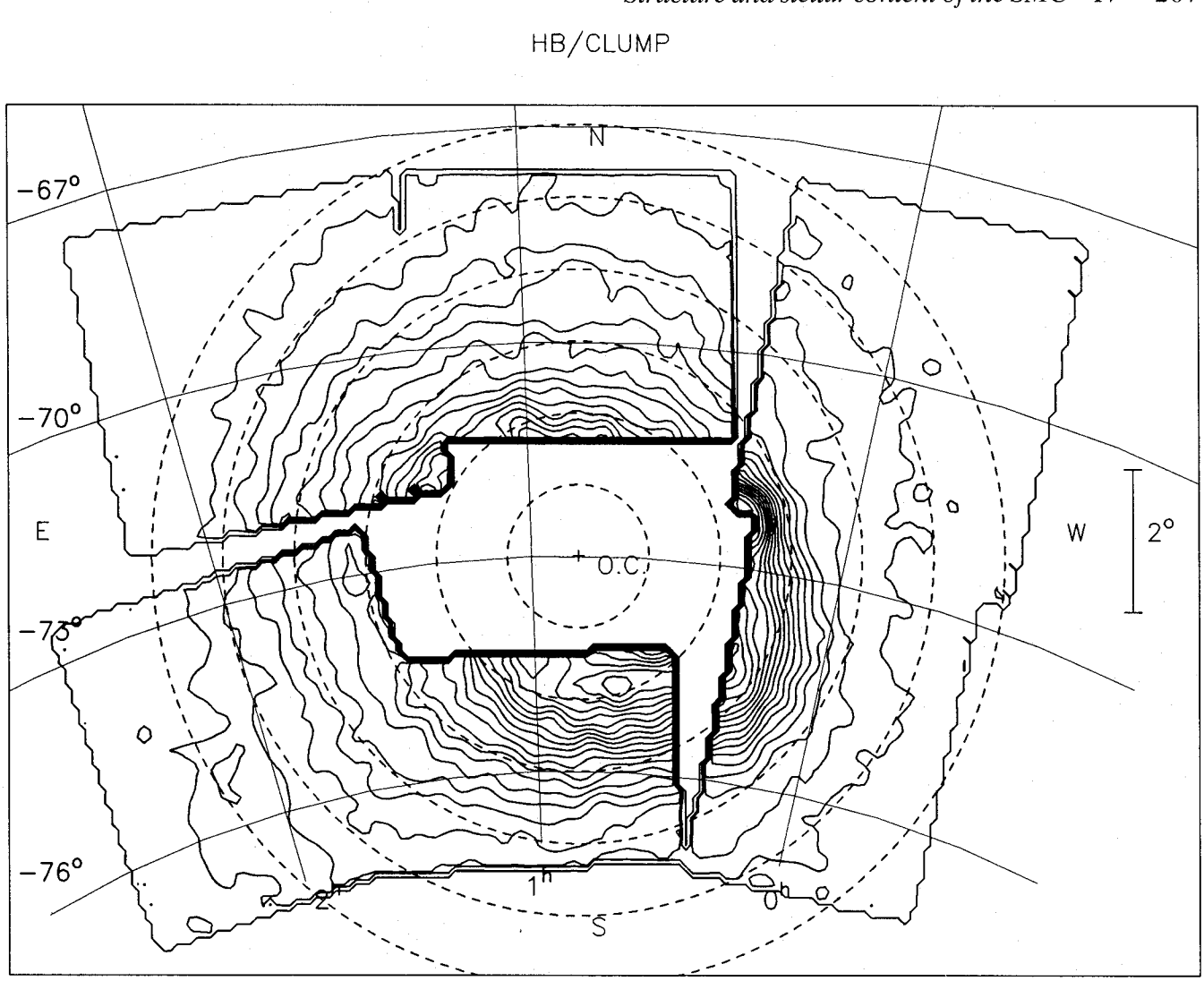

Figure 8. Contour plots of the surface distribution of HB/clump stars defined by the colour–magnitude limits $0.6 < B-R < 1.8$, $18.2 < R < 19.5$ for all six survey fields. Concentric radii at 1°, 2°, 3°, 4°, 5°, 6° from the SMC optical centre are shown. The contour levels increase towards the SMC centre and consist of levels of 9, 13, 17, 21 ... stars per pixel. The contribution from galactic foreground stars is about 7.5 counts per pixel. To obtain the number of stars per square degree, multiply by 115. The galactic globular cluster 47 Tuc is located about 2° to the WNW of the optical centre, distorting the number counts in its vicinity.

4.1 The surface distribution of clump/red-horizontal-branch stars

The technique applied here is identical to that used in Section 3 for the production of the surface distribution of MS stars. The full data base from all six survey fields was used for the construction of the contour map presented in Fig. 8. All stars within $18.2 < R < 19.5$ and $0.6 < B-R < 1.8$ were counted as belonging to the HB/clump. The luminosity limits were selected on the basis of the larger apparent luminosity range of clump/HB stars in areas with large geometrical depths (see Papers II, III), while the colour limits were selected to include, as well as the HB/clump, the yellow galactic foreground ridge lying superimposed on the HB/clump in the given luminosity range. This was done to avoid fluctuations in the statistics due to systematic photometric zero-point drifts from field to field.

There is a contribution from the galactic foreground stellar population of approximately 7.5 counts per pixel due to their inclusion within the colour and magnitude limits used for selecting the clump stars. In addition, red giant branch stars are also included in the clump number counts since the red giant branch locus intersects the clump feature on the CMD. Their numbers amount to about 40 per cent of the clump numbers over the range of magnitudes used to define the clump population. This figure has been calculated from the number–magnitude histogram of clump stars after subtraction of the galactic foreground contributions (see Papers II, III for examples of histograms). Cannon (1983) has pointed out that the ratio of the numbers of stars in the upper red giant branch to those in the HB phase may depend on the age of the stellar population. However, studies of the ratio of the numbers of stars in the upper red giant branch to those belonging to the HB/clump as a function of position in the

SMC using our data base (details are described by Hatzidimitriou 1989 pp. 143, 144) showed no systematic variations of this quantity. The same work also showed, from published data on Magellanic Cloud clusters, that this ratio is not a sensitive indicator of age for clusters older than 1–2 Gyr.

The surface distribution of the HB/clump appears somewhat irregular, with the inner contours displaying a different shape to the outer contours. Essentially, the inner contours appear to describe an elliptical shape out to about 3°–4° from the SMC centre, with the major axis of the ellipse aligned roughly with the position angle of the SMC major axis (de Vaucouleurs 1955). The outermost contours appear to be more nearly circular than the inner contours, but the shape still deviates significantly from radial symmetry.

4.2 Age estimates for the bulk of the SMC field population

4.2.1 Contribution to the clump/red-horizontal-branch stars from populations younger than 1–2 Gyr

As mentioned in Section 3, the MS stars detected on the CMDs span an age range from a few 10^8 yr (or younger in the Wing region) to probably $\simeq 2$ Gyr. We now investigate the extent to which the observed numbers of clump/red-HB stars can be interpreted as originating in these younger populations. It is obvious from a comparison of the contour plots of Figs 8 and 5 that the clump stars have a more extended distribution than the stars younger than 2 Gyr, as represented by the observable MS stars. Therefore the clump includes a significant proportion of stars older than this limit.

First, we consider whether any contribution to the clump would be expected from the very young (<0.1 Gyr) stars of the SMC Wing. Cannon (1970) and Mateo & Hodge (1985) find that, for galactic open clusters younger than $3\text{–}5\times10^8$ yr, the 'clump' due to core helium burning stars becomes rapidly brighter with decreasing age, in agreement with theoretical models (e.g. Faulkner & Cannon 1973). Inspection of the colour–magnitude diagrams of galactic open clusters compiled by Mermilliod (1981a) in conjunction with the ages determined by Mermilliod (1981b) show that the 'clump' of red giants is fairly well defined between ages of 0.6 and 0.2 Gyr, but at about 0.1 Gyr it becomes less concentrated until its existence is very doubtful at an age of 0.05 Gyr. If the stellar population of the Wing is about the same age as the Pleiades open cluster with an age of about 0.08 Gyr, a loosely defined 'clump' feature would be expected at around $M_R=-3$ or $R=16$. The fact that no such feature could be identified in the CMDs in the Wing region (see Appendix B) seems to confirm our age assignment of 0.05 Gyr made for the Wing feature in Section 3.

As discussed in Paper II, populations aged between 0.5 and 10 Gyr possess a clump of core helium burning red giants whose mean magnitude is largely independent of age and metallicity, and hence, for areas possessing MS populations outside the Wing, clump stars coeval with the detected MS populations would be expected at approximately the same luminosity level as populations older than 2 Gyr. In order to investigate the contribution of populations aged less than 2 Gyr but older than 0.4–0.5 Gyr to the total population present in areas with significant MS populations, we use, as a first approximation, the formula derived by Cannon (1970) for the lifetimes of stars in different evolutionary phases, except that we will assume that the lifetimes are known and use the equation to predict the numbers of clump stars due to populations coeval with the young MS populations. The equation is

$$\frac{\Delta t}{t}=0.74\,\frac{N}{N_0}, \qquad (2)$$

where Δt is the HB/clump lifetime, t is the age of the stellar population, N is the number of clump stars and N_0 is the number of stars per unit magnitude range in the section of the zero-age main sequence (ZAMS) from which the progenitors of the clump stars were derived. Following Cannon (1970) we assume that the progenitors of the clump stars came from the section of the MS 0.5 mag above the MS turn-off and that the LF of the ZAMS is flat in this region, a reasonable approximation given the shape of the Wing LF used to derive an 'initial LF' in Section 3. We adopt the HB/clump lifetime found by Cannon of about 2×10^8 yr, which agrees roughly with the lifetimes obtained from the theoretical models of Seidel, Demarque & Weinberg (1987) whose evolutionary tracks for the HB/clump phase cover about 1×10^8 yr. We have evaluated the contribution to the clump for two areas, namely the 'inner' region of Field 52 within $2°<r_{oc}<2\overset{\circ}{.}5$, and the outer region in Field 52 within $2\overset{\circ}{.}5<r_{oc}<4°$. The results given by the above equation are sensitive to the assumed age of the stellar population. For the inner region the age of the dominant population is fairly well defined (0.4–0.6 Gyr), and we have counted the numbers of MS stars in the section between $R=18.0$–18.5 which presumably represents the half-magnitude below the MS turn-off. Since we have assumed a flat LF, this is also the number of stars on the unevolved MS 0.5 mag above the top of the MS from which the clump stars originated. For the outer region, we have assumed an age of about 1 Gyr but, as stated earlier, there is no dominant age contribution. Since older stars contribute to a steep observed LF, the MS counts for population aged less than 1 Gyr will have been overestimated, giving an upper estimate of the <1 Gyr contribution to the clump.

Table 4 shows the relevant data for the calculation of the contribution of fairly young populations to the clump. It can be seen that, for the outer region, this contribution is exceedingly small, of the order of a few per cent, and even in the inner regions the contribution only rises to about 14 per cent of the total clump numbers. For the outer region, if we were to assume a dominant age of 1.5 Gyr rather than 1 Gyr and

Table 4. Data for the study of the contribution of <2 Gyr populations to the HB/clump in two circular grid regions in Field 52. See text for details.

	F52:Inner	F52:Outer
Inner/Outer radii (deg.)	2/2.5	2.5/4
Assumed age (Gyr)	0.4	1.0
Count range (R mag)	18.0 – 18.5	19.0 – 19.5
Number per unit mag, N_o	266	548
Calculated contribution to clump, N	180	148
Observed number in clump	1322	6272
Percentage contribution	14	3

count the numbers of MS stars in the range $R = 19.5$–20.0, the result would still be only 4 per cent for the contribution to the observed clump numbers, although this number is affected more by incompleteness towards faint magnitudes. These figures give some indication of the absolute contribution of these younger populations to the total stellar population beyond 2° from the SMC centre, and show conclusively that it consists largely of populations older than about 2 Gyr.

4.2.2 *Contribution to the clump/red-horizontal-branch stars from populations older than 2 Gyr*

As was demonstrated in the previous paragraph, less than 15 per cent of the clump population can be ascribed to stars younger than 2 Gyr, hence the bulk of the underlying population is older than $\simeq 2$ Gyr. We shall attempt now to use the clump/red-HB structure to analyse further its age constitution.

The main method that will be used for this purpose was recently discussed by Hatzidimitriou (1991, H91), and involves a new age index, d_{B-R}, defined as the difference between the median colour (in $B-R$) of the clump/red-HB and the colour of the red giant branch at the level of the HB. The age dependence of this index was investigated both empirically (using several well-studied open and globular clusters in our own Galaxy and in the Magellanic Clouds) and theoretically using the Seidel *et al.* (1987) clump/red-HB models in conjunction with the revised Yale isochrones (Green, Demarque & King 1987). Empirically, there is a well-defined linear correlation between d_{B-R} and age, given by the equation (Hatzidimitriou 1991):

$$d_{B-R} = 0.08 \pm 0.01 + (0.015 \pm 0.001) \times (\tau/\mathrm{Gyr}). \quad (3)$$

This age calibration scheme is applicable to populations with purely red HBs, older than 1–2 Gyr and with metal abundances ranging from $[\mathrm{Fe/H}] = -1.7$ to solar. It is independent of reddening, distance modulus and systematic errors in the photometry, and it is largely insensitive to metallicity within the age and metallicity ranges mentioned above.

It should be emphasized here that the age estimates derived for mixed populations using the d_{B-R} index correspond to the median age of the mixture, which may be strongly biased by the age of the dominant population, if such a dominant population exists. In the following, the index d_{B-R} will be used to estimate the ages of the dominant populations in the SMC general field.

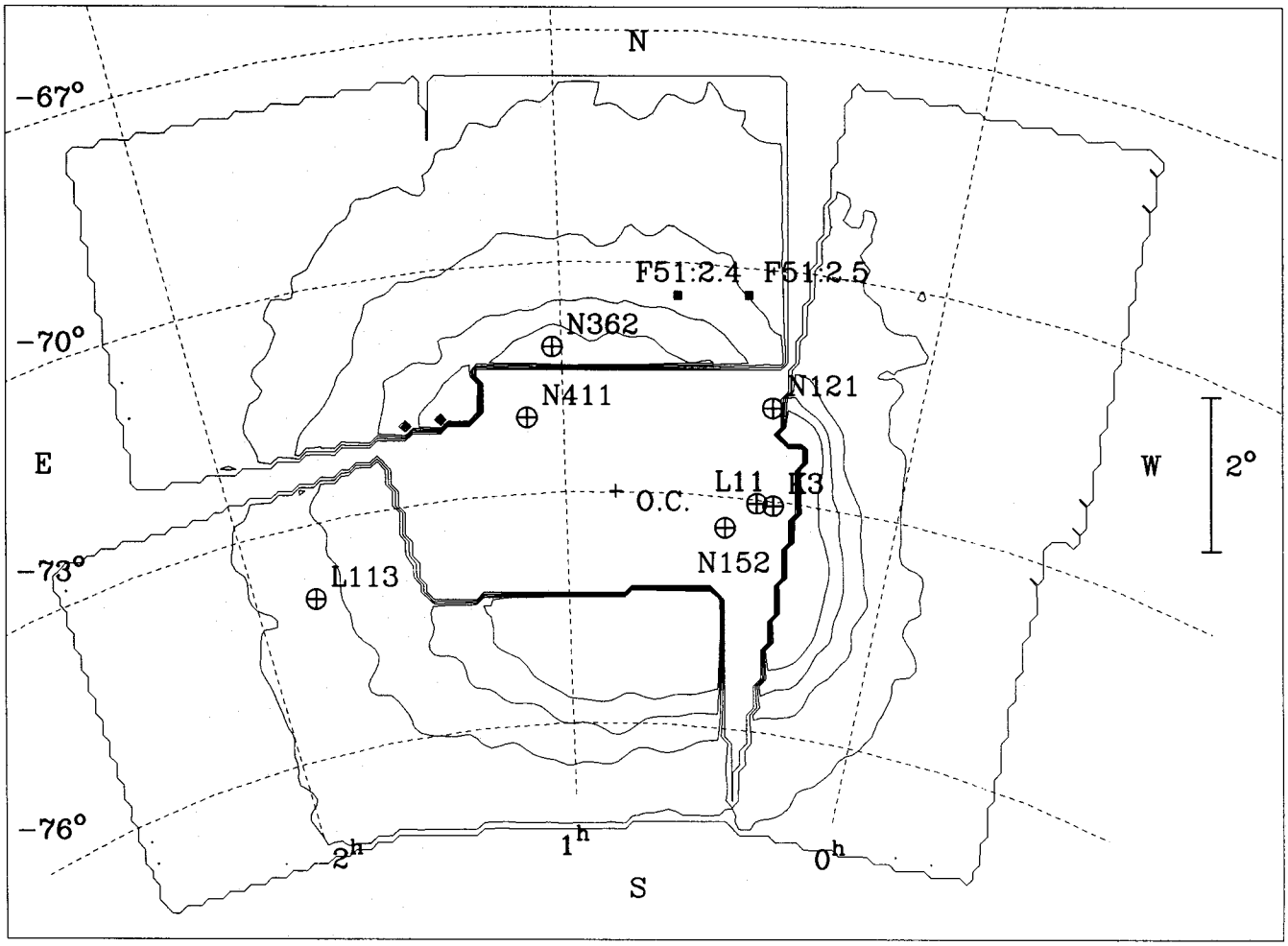

Figure 9. Locations of clusters and field regions referred to in Section 3, superimposed on the contour plot of the surface distribution of HB/clump stars. The contour levels increase towards the SMC centre and consist of levels of 12, 24, 36, 48 stars per pixel with a galactic foreground contribution of 7.5 stars per pixel.

First, the method is applied to all existing good-quality CCD CMDs of SMC field regions, all located near well-studied clusters, for which the index d_{B-R} can be defined. Table 5 lists the regions, their distance from the optical centre of the SMC, the derived value of d_{B-R} and the corresponding median age from the application of equation (3).

Table 5. Column 1 gives the name of the cluster near which the SMC field region lies, column 2 gives the projected radial distance in kpc of the region from the optical centre, column 3 gives the estimated value of d_{B-R}, and finally column 4 gives the estimated median age of the field derived from $d_{B-R}=0.08\pm0.01+(0.015\pm0.001)\times\tau$(Gyr) (see H91). The typical estimated error for d_{B-R} is ±0.04, which corresponds to an uncertainty in the estimated median age of the order of ±2.5 Gyr.

Region	r_{oc}(kpc)	d_{B-R}	$<\tau>$(Gyr)
NGC121	2.3	0.25	11
NGC152	1.5	0.12	3
NGC362	2.2	0.22	9
NGC411	1.5	0.14	4
L11	2.3	0.22	9
L113	4.2	0.23	10
K3	2.0	0.19	7

Note: the references for the field CMDs can be found in Table 1.

Fig. 9 indicates the location of the regions on the contour plot of the clump stars and in Fig. 10 we have plotted the derived median age against distance from the SMC optical centre. An inspection of Table 5 shows that, except for the innermost areas near clusters NGC 411 and 152 which have a median clump age of about 4 Gyr, most other areas have median ages between 9–11 Gyr. The region near Kron 3 has an intermediate value of 8–9 Gyr. This rapid increase of the median clump age within the central 2°.5 (see Fig. 10) is consistent with faster decrease of the younger populations than the older ones with distance from the centre.

Now we move to the outer contours of Fig. 9, where there are no CCD CMDs available and therefore we have to rely on the photographic data presented here. Although the definition of the index d_{B-R} does not require deep CMDs, it does require reasonably good photometric accuracy in the red giant and HB region of the CMD, and a well-delineated red giant branch. As can be seen in Appendix B, these two requirements are not always met in the present data base. However, in all cases where d_{B-R} could be defined in our CMDs, values comparable – within the errors – to those found near NGC 121 and L113 (about 10 Gyr) were found. These areas do not reach the outermost contour of Fig. 9, where d_{B-R} could not be reliably defined.

4.3 The oldest populations

4.3.1 Red horizontal branch structure

It is well known that the structure of the HB of older populations (possessing ages similar to the ages of globular clusters), i.e. whether it is purely red, or whether it extends to the instability strip and beyond, depends on metallicity as well as on several other possible parameters (candidates for the so-called 'second parameter'). Metallicity is the dominant 'first

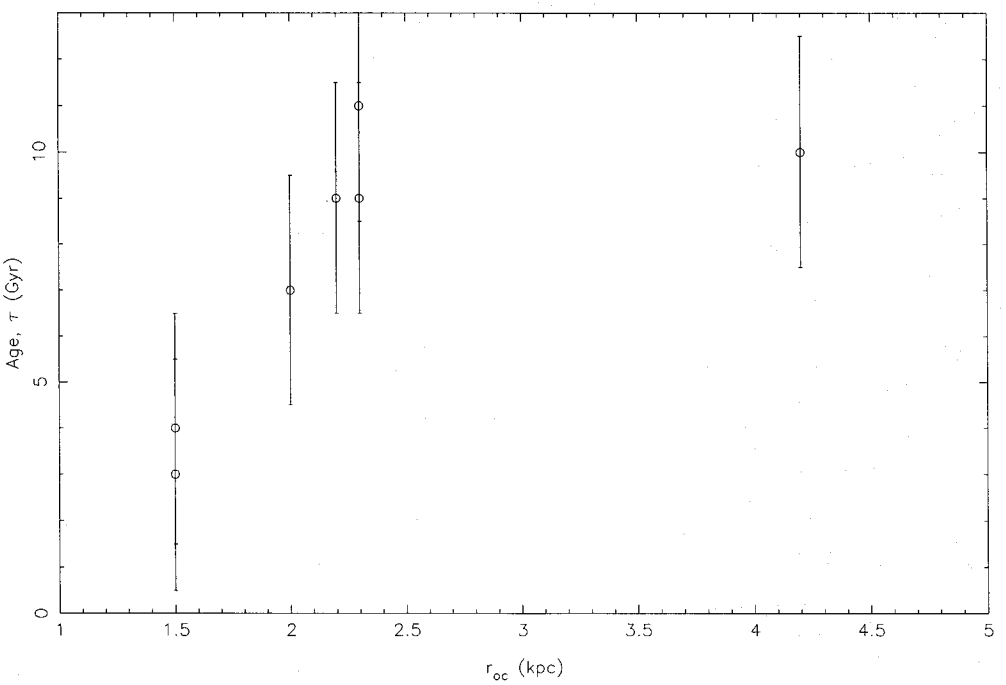

Figure 10. Median age versus distance from SMC optical centre for field regions located near clusters studied with CCD photometry (see Table 5 for data). The median age was derived using the d_{B-R} indicator as described in the text.

parameter' since, in general, metal-poor galactic globular clusters exhibit blue HBs while metal-rich ones are observed to possess red HBs. However, the HB structure of globular clusters beyond 12 kpc from the Galactic Centre is not well correlated with metallicity (Searle & Zinn 1978), hence the necessity for the second parameter to explain the HB structure. Nevertheless, no *extremely* metal-poor ([Fe/H] ~ −2.0) globular clusters are seen to have a purely red HB. For the present analysis we note that old galactic globular clusters with purely red HBs have metallicities between [Fe/H] = −0.7 (47 Tuc) and −1.7 (Palomar 4), and that old giants in the SMC halo have metallicities of about [Fe/H] = −1.6 ± 0.3 (Suntzeff *et al.* 1986). Therefore, unless a 'second' parameter is in play, SMC populations as old as 15 Gyr – if present – may exhibit red HBs.

We now analyse in detail the red HB in the 'best' CMDs of our sample. These CMDs were chosen on the basis of several criteria, including good photometric accuracy (which is a function of the number and the quality of the plates combined to give B and R magnitudes), the existence of a well-delineated red giant branch, and a small clump magnitude range indicating a relatively small line-of-sight depth in the region. Region 2.4 in Field 51 from Paper III (see Appendix B) was selected for analysis.

A close inspection of the CMD F51:2.4 shows that there is an apparent asymmetric extension of the main clump to hotter temperatures. For a convincing analysis of the clump/HB region we need to remove the contributions of the red giant branch (which mostly affects the main clump) and foreground stars (which affects the asymmetric blue extension). The method chosen is as follows: a series of magnitude histograms between $18 < R < 20$ were constructed in 0.1-mag colour strips covering the range from $B-R = 0.7$ to 1.6. In each of these histograms, the foreground plus red giant branch contribution was defined and the adopted number subtracted from each bin. The remaining stars are treated as 'real' clump/HB stars. Table 6 shows the total number of clump/HB stars in each colour bin along with the corresponding mean magnitude of the stars.

First, we notice that, even after the removal of the foreground plus red giant branch contributions, there are still some HB stars reaching colours as low as $B-R = 0.7$. Secondly, the mean magnitude of the clump/HB stars becomes brighter with increasing colour by roughly 0.15 mag. This change does not happen in a continuous fashion, but rather in a step, with the first three colour bins having a systematically fainter mean magnitude than the last eight bins. We know from the clump/red-HB models of Seidel *et al.* (1987) that the mean magnitude of the red HB becomes fainter with increasing age, the rate of decrease in the luminosity being significantly greater for clump masses smaller than 0.9 $M_{\odot}$, or ages larger than ≃ 10–13 Gyr. Therefore the above observations may indicate the presence of a population older than the dominant ones represented by the well-populated 'main' clump.

Turning to the colour distribution of the clump/HB stars as derived from Table 6, we note the asymmetric tail towards bluer colours. All of the stars in the colour bin 1.0–1.1 and a large proportion of the stars in the 0.9–1.0 bin can be interpreted as higher error points from the main clump peak. Most of the stars in the 0.7–0.8 and 0.8–0.9 bins, however, are genuinely 'bluer' red HB stars. The total number of these

Table 6. The mean R magnitude of clump/red-HB stars (column 2) in the indicated (column 1) colour intervals, for the region F51:2.4. The mean R magnitude was calculated after removing the foreground and red giant branch contributions as explained in the text. Column 3 gives the number of clump/HB stars in each colour bin.

(B–R)	$< R >$	n
0.7-0.8	19.14	23
0.8-0.9	19.23	32
0.9-1.0	19.04	61
1.0-1.1	19.01	91
1.1-1.2	18.96	293
1.2-1.3	18.97	344
1.3-1.4	18.97	232
1.4-1.5	19.00	152
1.5-1.6	19.00	50
1.6-1.7	18.98	12

'bluer' red HB stars in this area, after accounting for the contribution from high-error points from the main clump, is of the order of 100, while the number of stars belonging to the main clump is about 1100. The mean colour of the 'bluer' red HB stars is $B-R \simeq 0.9$, while the main clump has a mean colour of $B-R \simeq 1.25$. The mean colour of the red giant branch at the level of the HB is about 1.5. This value is interpreted as representing the red giant branch of the dominant populations. The blue edge of the red giant branch is used for the 'older' populations (in order to derive a lower limit for d_{B-R}), giving a value of 1.25 for $(B-R)_g$. Thus we derive a value of 0.25 for the index d_{B-R} for the main clump/HB, and a value of ≃ 0.35 for the 'bluer' HB. The first value is comparable to the value derived from CCD CMDs near NGC 121 described above, and corresponds to an age of 10–12 Gyr (from equation 3). The second value is comparable to the values derived for the old galactic globular clusters with purely red HBs (like 47 Tuc, Pal 4 and Eridanus).

From the previous discussion it can be concluded that these older stars are an order of magnitude (≃ 9 per cent from the numbers given above) less frequent than the dominant population with a median age of 10–12 Gyr. Interestingly, Frogel (1984) has concluded that the old population which is responsible for the field RR Lyrae stars near NGC 121 amounts to approximately 6 per cent of the total mass in that area. This number is not incompatible with our estimate for the 15–16 Gyr old population. To convert the 9 per cent mentioned above to relative mass involved in the two groups, we need to take into account the relative lifetimes in the red HB as a function of age as well as the difference in the mass of the stars. From the models of Seidel *et al.* (1987) we conclude that the first of these factors is very

near unity. The second factor is about 0.8 (from Yale isochrones, for example), bringing down the estimated relative contribution to total mass of the two systems to $\simeq 7$ per cent.

The presence of a population at least as old as 12 Gyr is, of course, also indicated by the presence of RR Lyrae stars in the SMC general field. This lower age limit for RR Lyrae variables is defined by the age of the cluster NGC 121 which is the youngest known cluster to possess RR Lyrae variables (GC5). What we have achieved here is to push the lower age limit for the SMC general field to higher values by suggesting that stars as old as 15–16 Gyr are very likely to be present. This analysis has assumed that the d_{B-R} age indicator is applicable to SMC field populations, which has been confirmed by checking its relationship with other indicators of relative age (see H91).

4.3.2 *Blue horizontal branch stars*

The general field in both the SMC and the LMC is not known to contain blue HB stars. Although in the LMC there are a few star clusters with a blue HB (like Hodge 11 and NGC 2257), there are no such clusters in the SMC. Because of the still unknown factor of the 'second parameter' which affects the horizontal branch structure, it is not yet clear whether this apparent absence of blue HB stars in the SMC is due to higher metallicity (first parameter), lower age (one of the second parameter candidates), or some other factor. Metal enrichment may have happened quite fast in the Magellanic Clouds (as in our own Galaxy), in which case the numbers of very metal-poor old stars that would contribute to a blue HB population may be very low. The present study, because it covers large areas of the SMC field region, can be used to set statistical upper limits on the numbers of such stars.

A blue HB similar to the one found in the CMD of the LMC cluster Hodge 11 (Stryker *et al.* 1984; Andersen, Blecha & Walker 1984) would occupy a region in a SMC field CMD roughly within the limits $19 < R < 20$ and $B - R < 0.1$. Although there is not much foreground contamination in this part of the CMD, there are varying numbers of MS stars. An additional problem is the increasing incompleteness of our survey beyond $R = 19.5$, as can readily be seen in the MS luminosity functions presented in Section 3.

A first inspection of the CMDs of Appendix B shows that there is no conspicuous contribution of the blue HB in the general population. In the higher star number density areas (nearer the central parts of the SMC) the blue HB would appear as a bump in the MS LF at about $R = 19.5$ mag, if sufficiently well populated; the apparent peak of some LFs at about 19.5 mag (Section 3.3) is easily explained as a result of incompleteness. In the lower star number density regions, the statistics are poor, albeit the contribution of MS stars becomes less important. In these regions we combined CMDs from several grid regions to improve the statistics, but were still unable to find any definable blue HB. An upper limit of 10 blue HB stars per square degree, subject to increasing incompleteness towards faint magnitudes, is obtained using the colour–magnitude limits defined above on the combined CMDs, indicating that blue HB stars, if they exist at all, are an order of magnitude less frequent than the old (~ 15 Gyr) red HB stars.

5 DISCUSSION

5.1 Population group studies in the SMC

Studies of different population groups have aided the tracing of the age distribution in the SMC, but have generally lacked the large areal coverage of the present study. Here, we augment our understanding of the age distribution by means of comparison with these studies.

Azzopardi & Rebeirot (1991) have summarized the properties of the distributions of several population groups including young populations (less than a few 10^8 yr) such as late- and early-type supergiants, Hα emission-line stars and small nebulae, and intermediate-age population groups such as carbon stars and planetary nebulae. It is evident that the younger populations are concentrated in the Bar of the SMC and in the Wing, with the older age groups apparently less centrally concentrated but still possessing an elongation along the axis of the Bar in the NE–SW direction. This general pattern can be compared with the elongated and highly centrally concentrated distribution of the younger (0.3–0.6 Gyr) MS populations along the SMC major axis (see Figs 5 and 7) and the less centrally concentrated distribution of the older HB/clump population (Fig. 8). A more detailed comparison of the HB/clump surface distribution with that of the carbon stars, whose ages range from about 0.8 to 8 Gyr (see e.g. Iben 1984) and therefore overlap with the ages of HB/clump stars, is instructive. As noted in Section 4.1, the HB/clump distribution in the inner parts appears to be elliptical in projection with its major axis aligned in a NE–SW direction. On closer inspection the centre of this distribution appears to be located about half a degree to the SW of the optical centre. The corresponding carbon star distribution based on continuous star counts is also elongated along the SMC major axis and its centroid is displaced to the south of the optical centre. Although it is not clear that the two distributions are due to coeval populations, the similarities between the distributions suggest that they may share a common structural interpretation. The kinematical study by Hardy, Suntzeff & Azzopardi (1989) of a sample of carbon stars is consistent with the conclusion that the carbon stars belong to a kinematical spheroidal population. The outermost HB/clump contours are more circular than the inner contours and therefore this elliptically shaped component appears to be confined to the more central areas not beyond 4° from the optical centre.

The properties of the SMC cluster distribution should also be mentioned here. Van den Bergh (1991) has noted the concentration of young clusters in the SMC Bar and the more dispersed distribution of the older clusters, again following the general pattern described in the previous paragraph. Brück (1975), however, from a larger cluster sample but using more subjective age-dating criteria, locates the centroid of the oldest clusters somewhat to the SW of the optical centre, an observation which coincides with the displacement of the inner elliptical HB/clump component, representing the older stellar populations, to the SW. Da Costa (1991) has described the age distribution and age–metallicity relation for Magellanic Cloud clusters which have been studied down to the MS turn-off. For the SMC, it is clear that production of clusters has been more or less continuous over the last 10–12 Gyr, with no favoured epoch.

Although the star formation history in the general field may differ from the history of cluster formation, the uniform age distribution of SMC clusters indicates that star formation has been occurring at significant levels in parts of the SMC outer regions throughout the past 10 Gyr. The age composition in the general field in the outer areas has been shown by deep CCD colour–magnitude diagram studies near clusters (see Table 1) to be dominated by populations aged about 10 Gyr, often in contrast to the embedded (in projection) clusters, which are generally younger (e.g. G2, G3). This result on the age of the bulk of the field populations in the outer regions is in agreement with our conclusions on the median age of populations derived by using the d_{B-R} indicator in Section 4.

The projected distributions of old stellar populations (≥ 10 Gyr) such as old long-period variables and RR Lyrae stars in the SMC have not been comprehensively studied. Graham (1975, 1984) has studied RR Lyraes in two sample areas near the galactic globular clusters 47 Tuc (in the north-west) and NGC 362 (in the north), finding that these populations do not display a strong central concentration and that they appear to be preferentially located towards the western part of the SMC. The weak central concentration of RR Lyraes possibly indicates that they have a spheroidal distribution. The fact that the outer HB/clump contours are roughly circular supports the idea of a quasi-spherical halo component in the SMC. Since we cannot isolate the surface distribution of the oldest populations on the basis of our colour–magnitude data, further study of the oldest populations will have to rely on these variable star populations.

5.2 Comparison with the LMC age distribution

In the LMC, although a number of globular clusters similar in ages to galactic globular clusters and possessing RR Lyraes and/or blue horizontal branches exist, the general field in the LMC is believed to be younger in the mean than that of the SMC. Studies by Stryker (1984a), Stryker & Butcher (1981), and more recently by Hodge (1987b) have shown that, out to 9° from the LMC Bar, the dominant population is of intermediate age. The latter two studies investigated fields within 5° of the LMC Bar and found evidence for a dominant population component aged 2–4 Gyr which may indicate that a burst of star formation occurred in this epoch. The more remote area lying 9° NE of the LMC Bar, studied by Stryker (1984a), indicated the presence of a 7-Gyr field population at least several Gyr younger than the nearby old LMC globular cluster NGC 2257. A median age of 7–9 Gyr was also derived by H91 for the field population near the cluster Hodge 11, in good agreement with Stryker's result. There is thus a strong possibility that the dominant populations in the general field in the LMC are at least 2–3 Gyr younger in the mean than the dominant field populations in the SMC, whereas towards the remote outlying areas of the LMC the ages of the dominant field populations may converge to that of the SMC outer regions.

The cluster formation history of (at least the more massive) clusters in the two Clouds also seems to be diverse. The age distribution of LMC clusters (Da Costa 1991) shows a conspicuous gap between 4 and 15 Gyr, populated by only one cluster. In contrast, the SMC has a few clusters in this age range. Moreover, the age–metallicity correlations for clusters in the two Clouds appear to differ (Da Costa 1991); the SMC clusters have essentially the same mean metallicity for 8–9 Gyr, while the LMC age–metallicity relation may be monotonically increasing. Stryker & Butcher (1981) suggested that the major burst of star formation about 4 Gyr ago in the LMC may have been triggered by a close approach to the Galaxy, but the disparate nature of the age distributions between the Magellanic Clouds of both cluster and field populations is not easily explained if they are assumed to be bound to each other over most of their history.

In all field areas studied in the LMC, no trace of a horizontal branch lying on the blue side of the instability strip has been found, despite the fact that globular clusters with blue HBs exist. As stated in Section 4, no blue HB population was found in the SMC either. Thus the early histories of the two Clouds may be similar in that a very brief initial burst raised the metallicity to about $[Fe/H] = -1.8$, and the lack of observed blue HB stars may be explained if we assume that metallicity is the main parameter controlling the structure of the horizontal branch for very old populations. In the SMC, no clusters were produced in this initial burst, whereas several were produced in the LMC. The lack of these SMC clusters is in itself not surprising on statistical grounds if the numbers of these clusters were proportional to the galaxy mass. Only 1–2 such clusters in the SMC would be expected, given LMC and SMC masses of 6 and $1.5 \times 10^9\ M_\odot$ respectively.

5.3 The nature of star formation processes in the SMC outer regions

In this subsection we consider the processes responsible for star formation in the outer parts of the SMC. As an irregular galaxy it may be expected to display a disordered pattern of star formation, but the role of interactions with the Galaxy and the LMC might also be important. Various authors (see e.g. Stryker 1984b; Westerlund 1989, 1991) have tried to establish whether star formation in the Magellanic Clouds has proceeded continuously or primarily in bursts. The former possibility excludes the idea that the generations of stars were created as a result of star formation mostly precipitated by external interactions, since close tidal encounters are of limited duration and may be periodic events. The latter possibility, however, does not necessarily exclude internal processes as the cause of major star formation episodes.

From the results presented in the previous sections we can attempt to answer the following questions which are related to this discussion.

(1) Do we have evidence for bursts of star formation in the SMC outer regions?

(2) What can we say about the nature of star formation processes in the Magellanic Clouds from a comparison of their star formation histories?

(3) What evidence do we have to support the view that external interactions have stimulated star formation in the SMC?

(4) Is there evidence to indicate that recent tidal interactions have modified the observed population structure in some parts of the SMC?

The following discussion focuses on these points in turn.

(1) Aside from the clear-cut example of the Wing region, which will be discussed in more detail later, our direct observational evidence for bursts of star formation in the SMC outer regions is not conclusive, being hampered by the fact that we only have good time resolution up to about 2 Gyr ago. As discussed in the previous subsection, the majority of stars in the outer regions of the SMC appear to have been formed in one major burst or enhanced star formation phase of unknown duration about 10 Gyr ago, and further progress on this question will depend on more extensive deep observational data. The best supporting evidence we have for an enhancement in the star formation rate in any region over the past 2 Gyr is the well-defined break in the LF at about $R = 18$ in the LFs for the inner regions within 2°.5 of the SMC centre in Fields 51 and 52, implying the existence of a population component aged about 0.4–0.6 Gyr, depending on the distance modulus. This result suggests that the star formation rate was comparatively low for at least 1 Gyr prior to this time. These areas are located near the edge of the northern outer arm and Brück (1980) also suggests that star formation in these areas was due to a bursting star formation mode.

No distinct period of star formation could be identified from the MS LFs of the outer regions studied. The steep LFs in the outer regions of Fields 52, 51 and 29 indicate that the star formation rate has been decreasing with time over the past 2 Gyr or so in these areas and is currently at insignificant levels. It is possible that we are observing the tail end of a star formation episode begun shortly before 2 Gyr ago, or that star formation has been decreasing continuously over a much longer period of time. Observations to fainter magnitudes are required to determine whether there is a 'break' in the LF corresponding to the start of a definite epoch of star formation.

(2) The ages of the generations of stellar populations in the SMC and the LMC should provide clues to the nature of star formation processes which gave rise to them. In particular, as remarked by other authors (e.g. Westerlund 1989; Da Costa 1991), if these ages were found to match each other closely for the LMC and the SMC, this would constitute strong supporting evidence that their common interactions with the Galaxy and each other have stimulated star formation in both Magellanic Clouds. However, the situation appears to show the contrary; as discussed earlier, the ages of the major generations of stars and the age distribution of clusters in the two Magellanic Clouds show considerable differences. The tidal models of the interactions of the Galaxy–LMC–SMC system developed by Murai & Fujimoto (1980, see also Fujimoto & Murai 1984) suggest that the distance between the Magellanic Clouds and the Galaxy has been decreasing in an oscillatory manner over the past 10^{10} yr, which may indicate that only the comparatively more recent tidal encounters with the Galaxy have had a major influence on the star formation histories of the Magellanic Clouds. Another explanation is that the Magellanic Clouds have not existed in a binary state for most of their history. The possibility that they have only recently been captured by the Galaxy is favoured by Mathewson *et al.* (1987), but the nature of the binary state of the Magellanic Clouds has not been extensively studied. In short, the poor correlation between the star formation histories of the two Magellanic Clouds does *not* support the view that interactions of the Galaxy–LMC–SMC system are mainly responsible for the production of the various stellar generations in the Magellanic Clouds.

(3) Despite the negative conclusion of the previous paragraph, there is very strong evidence that *some* star formation in the SMC has been stimulated by external interactions; the SMC Wing region in particular is widely accepted as being due to an encounter. Its precise origin is uncertain; Irwin *et al.* (1990) consider that it resulted from a burst of star formation triggered by the near collision between the LMC and SMC about 200 million years ago predicted by Murai & Fujimoto (1980); Westerlund (1990), however, considers it to be part of the very young stellar generation seen in the Magellanic Clouds whose formation was perhaps triggered by the perigalactic approach of the Magellanic Clouds about 40 million years ago, also suggested by the Murai & Fujimoto models.

In the region dominated by the Wing feature, the *projected* distribution of the HB/clump representing the intermediate-age/old stellar population is relatively undisturbed, showing neither a pointed extension towards the LMC nor a clumpy distribution, whereas the MS distribution shows several concentrations and extends well beyond the outer HB/clump contours. This suggests that the Wing and the stellar link between the Clouds have formed from gas concentrations created from the action of ram pressure forces between the haloes of the Magellanic Clouds, rather than from tidally induced outflow of gas and other material from the central regions of the SMC. The age of the Wing feature (about 50 Myr) derived in Section 3 and that of the stellar associations in the inter-Cloud region (Grondin *et al.* 1990; Demers *et al.* 1991) seem to indicate, however, that star formation did not occur in these concentrations until precipitated by tidal perturbations due to the perigalactic passage of the Magellanic Clouds.

In order to assess the scale of the star formation burst in the Wing, we may perform a calculation to determine whether the numbers of stars created in the Wing represent a significant fraction of the total stellar population of the SMC. The calculation is based on the numbers of HB/clump stars that would be observed in the SMC in about 1-Gyr time, and a comparison of this number to the number of clump stars observed at present, which we assume will not have altered significantly 1 Gyr later. We adopt the technique employed in Section 4.2 to determine the contribution from the younger populations of the detected MS to the observed clump. The MS 'tip' luminosity for a 1-Gyr population for the Wing is $R = 19$, taking into account that the Wing appears to be located closer than the SMC main body with a difference in the distance modulus of 0.3 mag. Then the clump stars in 1 Gyr will have originally come from the section of the MS between $R = 18.5$–19.0. There are presently 2261 MS stars in this half-magnitude range in Field 30, and application of equation (2) with an HB/clump lifetime of 0.2 Gyr gives the result that a total of 1220 clump stars will exist due to the Wing feature beyond about 3° from the SMC centre in 1 Gyr. It can probably be assumed that the Wing 'feature' itself will be smeared out uniformly over the surface of the SMC as a result of orbital or dynamical mixing processes which operate on a time-scale of about 1×10^8 yr. This can be compared with a present number of about 65 000 true clump stars in all six survey fields located beyond 3° from the SMC

centre after having corrected for the galactic foreground and red giant branch contributions. Therefore the contribution of the Wing population to the present stellar content in the SMC outer area is about 2 per cent. Although the wing is a very prominent localized optical feature, it has thus not contributed much to the overall stellar content of the SMC, an analysis which concurs with our earlier discussion of the varied star formation histories of the two Magellanic Clouds. Nevertheless, the possibility that other, larger, bursts of star formation have been triggered by tidal interactions cannot be discounted, as conditions prevailing in the outer regions (such as the quantity of available gas) may have been very different in the past.

(4) The question of the effect of relatively recent tidal interactions on the population structure is raised by several observations from this paper and other studies. Observations reveal: (a) an asymmetrical distribution of (MS) populations younger than ~2 Gyr, but mainly older than ~0.5 Gyr, with respect to both the SMC centre and the distribution of the older stellar component represented by the HB/clump population (see Section 3); (b) large depths (~20 kpc) along the line of sight in the north-eastern (Papers II and III) and other eastern outer areas, generally coinciding with areas where extended distributions of MS stars are found, and (c) a correlation between distance and radial velocity indicated by a study of the NE outer area by Hatzidimitriou *et al.* (in preparation) (see also Hatzidimitriou, Cannon & Hawkins 1991), with the time-scale agreeing with the time of the recent (2×10^8 yr) LMC–SMC encounter according to the Murai & Fujimoto (1980) models.

The non-uniformity of the MS distribution for populations older than about 0.5 Gyr indicates that the origin of this distribution is fairly recent, given that orbital and dynamical mixing will have dispersed localized features on a time-scale of about 1×10^8 yr. Although the dissimilarity of the LFs between the inner and outer studied areas does not directly confirm that these outlying younger populations originated in the central areas, the most likely explanation for the above observations is that the relatively recent close encounter between the Magellanic Clouds, which appears to be responsible for the velocity structure and large depths in the north-east, *did* pull out stellar material from an area possessing populations aged between 0.5–2 Gyr. Since there is no evidence for a significant population component aged 0.5 Gyr or younger in the outlying areas, it seems possible that the external disturbance occurred before the formation of the younger (0.4–0.6 Gyr) stellar generation which dominates the inner areas of our study and possibly masks any older MS component. This requires the encounter to be located further back in time; the models of the Magellanic system developed by Mathewson *et al.* (1987) place the recent close encounter between the LMC and the SMC at 0.4 Gyr ago, compatible with our lower estimate for the major age component in the inner areas studied. Thus the disturbance due to tidal interaction with the LMC may account for the above observations, but more work must be done in order to define accurately the epoch of this disturbance and its consequences for the star formation history and dynamics of the SMC.

Finally, we discuss the internal processes which seem to be required to account for the bulk of the star formation in the Magellanic Clouds. As in the case of the Galaxy, the initial collapse of the protogalactic cloud may have produced the oldest stellar populations, but subsequent star formation processes may be similar to those thought to have operated in other irregular galaxies. In this regard, we note the existence of several isolated Magellanic irregulars, e.g. NGC 4449 (Bothun 1986), possessing clumpy distributions of sites of star formation and overall disordered optical appearance. Such galaxies are believed to have undergone star formation via a chaotic, free-wheeling mode unrestricted by dynamical forcing due to differential disc rotation (Gallagher & Hunter 1984). Gas mobility is probably an important factor in inducing star formation, either in the creation of local density fluctuations due to large non-circular motions in the gas component (Hunter 1982), or the propagation of star formation between neighbouring areas via expansion of H II regions, stellar winds and supernovae (stochastic self-propagating star formation). Models of stochastic self-propagating star formation have been developed by several workers and applied with some degree of success to irregular galaxies including the case of the Magellanic Clouds (see Gerola, Seiden & Schulman 1980). Kennicutt (1989), from studies of normal disc galaxies, established the reality of a critical threshold gas density for star formation, varying between galaxies and within individual galaxies depending on the rotation properties of the disc. For densities below the critical threshold the gas is stable to cloud-forming large-scale gravitational perturbations, whereas, above the threshold, gravitational instabilities can result in a star formation rate which increases rapidly with increasing density. The ageing towards the periphery of the SMC indicated by Fig. 10 suggests that, after successive generations of stars were created, star formation became progressively more concentrated towards the central regions of the SMC as the gas content of the outer zones became exhausted.

In conclusion, more theoretical and observational work is needed to evaluate quantitatively the interplay of internal processes and external stimulation in star formation, although the evidence reviewed here suggests that external interactions involving the SMC and its neighbours have played only a minor role in the overall star formation history in the outer regions of the SMC.

6 CONCLUSIONS

New results on the spatial/age distribution of the stellar content of virtually the entire outer area of the SMC have been obtained from COSMOS measurements of sets of blue and red UKST plates externally calibrated with CCD observations. Various techniques were employed to study the age composition and surface distribution of stellar populations, including surface distribution contour maps of main-sequence stars (for populations aged less than 2 Gyr) and horizontal-branch/clump stars (for populations between 2–10 Gyr), and analyses of main-sequence luminosity functions and horizontal branch structure.

A number of significant results have emerged from these investigations. The bulk of the field populations in the outer parts of the SMC (i.e. beyond 2–3 kpc from the SMC optical centre) has been shown to possess a median age around 10–12 Gyr. Colour–magnitude diagrams have shown the existence of a red horizontal branch similar to that of the galactic globular clusters 47 Tuc and Eridanus, from which

the existence of a very old 15–16 Gyr population can probably be inferred. Star count analysis shows that the contribution of this old population is about 7 per cent by mass of the total population in the outer regions of the SMC. No blue horizontal branch population with colours bluer than the RR Lyrae strip has been identified. The projected distribution of populations younger than about 2 Gyr has been shown to be non-uniform with respect to older populations, being biased towards the eastern side of the SMC. Comparison of the age distributions of the LMC and SMC, as well as star count analysis in the Wing region, suggest that star formation stimulated by interactions with the LMC and SMC plays only a minor role in the overall star formation history of the Magellanic Clouds.

The large areal coverage of this study has overcome the limitations of small-number statistics which had previously been a barrier to systematic investigations of the stellar age distribution in these outer regions. Nevertheless, further progress depends on the acquisition of data down to fainter magnitudes in the SMC field in order to reveal the detailed star formation history between 15 and 2 Gyr ago. The results presented here contribute to the overall picture of the age distribution in the outer regions by consideration of the more numerous populations represented in the main evolutionary phases, thereby extending the picture presented by less common but more accessible age tracers such as clusters, carbon stars and variable stars.

ACKNOWLEDGMENTS

The authors thank the UK Schmidt Telescope Unit for the loan of photographic plates, the COSMOS unit of ROE for plate measurements, and the Danish 1.5-m telescope facility at ESO for the opportunity to obtain CCD sequences to calibrate our photometry. We are grateful to M. Hawkins, G. Da Costa, R. D. Cannon and G. Meurer for helpful discussions, and to S. Demers and M. Irwin for computerized lists of their photographic photometry. LTG was supported by the SERC, and DH by an AAO–SERC fellowship.

REFERENCES

Andersen, J., Blecha, A. & Walker, M. F., 1984. In: *Structure and Evolution of the Magellanic Clouds, IAU Symp. No. 108,* p. 41, eds van den Bergh, S. & de Boer, K. S., Reidel, Dordrecht, Holland.

Azzopardi, M. & Rebeirot, E., 1991. In: *The Magellanic Clouds, IAU Symp. No. 148,* p. 71, eds Haynes, R. & Milne, D., Kluwer, Dordrecht, Holland.

Bolte, M., 1987. *Astrophys. J.,* **315,** 469 (GC6).

Bothun, G. D., 1986. *Astr. J.,* **91,** 507.

Brück, M. T., 1975. *Mon. Not. R. astr. Soc.,* **173,** 327.

Brück, M. T., 1980. *Astr. Astrophys.,* **87,** 92.

Buttress, J., Cannon, R. D. & Griffiths, W. K., 1988. In: *The Harlow-Shapley Symposium on Globular Cluster Systems in Galaxies, IAU Symp. No. 126,* p. 575, eds Grindlay, J. E. & Davis Philip, A. G., Kluwer, Dordrecht, Holland (GC8).

Caldwell, J. A. R. & Coulson, I. M., 1985. *Mon. Not. R. astr. Soc.,* **212,** 879.

Caldwell, J. A. R. & Coulson, I. M., 1986. *Mon. Not. R. astr. Soc.,* **218,** 223.

Cannon, R. D., 1970. *Mon. Not. R. astr. Soc.,* **150,** 111.

Cannon, R. D., 1983. In: *Highlights of Astronomy,* Vol. 6, p. 109, ed. West, R. M., Reidel, Dordrecht, Holland.

Da Costa, G. S., 1991. In: *The Magellanic Clouds, IAU Symp. No. 148,* p. 183, eds Haynes, R. & Milne, D., Kluwer, Dordrecht, Holland.

Da Costa, G. S. & Mould, J. R., 1986. *Astrophys. J.,* **305,** 214 (GC1).

Da Costa, G. S., Mould, J. R. & Crawford, M. D., 1985. *Astrophys. J.,* **297,** 582.

Demers, S. & Irwin, M. J., 1991. *Astr. Astrophys. Suppl.,* **91,** 171.

Demers, S., Grondin, L., Irwin, M. J. & Kunkel, W. E., 1991. *Astr. J.,* **101,** 91.

de Vaucouleurs, G., 1955. *Astr. J.,* **60,** 219.

de Vaucouleurs, G. & Freeman, K. C., 1972. *Vistas Astr.,* **14,** 163.

Faulkner, D. J. & Cannon, R. D., 1973. *Astrophys. J.,* **180,** 435.

Frogel, J. A., 1984. *Publs astr. Soc. Pacif.,* **96,** 856.

Fujimoto, M. & Murai, T., 1984. In: *Structure and Evolution of the Magellanic Clouds, IAU Symp. No. 108,* p. 115, eds van den Bergh, S. & de Boer, K. S., Reidel, Dordrecht, Holland.

Gallagher, J. S. & Hunter, D. A., 1984. *Ann. Rev. Astr. Astrophys.,* **22,** 37.

Gardiner, L. T. & Hawkins, M. R. S., 1991. *Mon. Not. R. astr. Soc.,* **251,** 174 (Paper III).

Gerola, H., Seiden, P. & Schulman, L., 1980. *Astrophys. J.,* **242,** 517.

Graham, J. A., 1975. *Publs astr. Soc. Pacif.,* **87,** 641.

Graham, J. A., 1984. In: *Structure and Evolution of the Magellanic Clouds, IAU Symp. No. 108,* p. 207, eds van den Bergh, S. & de Boer, K. S., Reidel, Dordrecht, Holland.

Green, E. M., Demarque, P. & King, C. R., 1987. *The Revised Yale Isochrones and Luminosity Functions,* Yale University Observatory, New Haven.

Grondin, L., Demers, S., Kunkel, W. E. & Irwin, M. J., 1990. *Astr. J.,* **100,** 663.

Hardy, E., Suntzeff, N. B. & Azzopardi, M., 1989. *Astrophys. J.,* **344,** 210.

Hatzidimitriou, D., 1989. *PhD thesis,* University of Edinburgh.

Hatzidimitriou, D., 1991. *Mon. Not. R. astr. Soc.,* **251,** 545 (H91).

Hatzidimitriou, D. & Hawkins, M. R. S., 1989. *Mon. Not. R. astr. Soc.,* **241,** 667 (Paper II).

Hatzidimitriou, D., Hawkins, M. R. S. & Gyldenkerne, K., 1989. *Mon. Not. R. astr. Soc.,* **241,** 645 (Paper I).

Hatzidimitriou, D., Cannon, R. D. & Hawkins, M. R. S., 1991. In: *The Magellanic Clouds, IAU Symp. No. 148,* p. 107, eds Haynes, R. & Milne, D., Kluwer, Dordrecht, Holland.

Hodge, P. W., 1987a. *Publs astr. Soc. Pacif.,* **99,** 724.

Hodge, P. W., 1987b. *Publs astr. Soc. Pacif.,* **99,** 730.

Hunter, D. A., 1982. *Astrophys. J.,* **260,** 81.

Iben, I., 1984. In: *Observational Tests of Stellar Evolution Theory, IAU Symp. No. 105,* p. 3, eds Maeder, A. & Renzini, A., Reidel, Dordrecht, Holland.

Irwin, M. J., Demers, S. & Kunkel, W. E., 1990. *Astr. J.,* **99,** 191.

Kennicutt, R. C., 1989. *Astrophys. J.,* **344,** 685.

Lequeux, J., 1984. In: *Structure and Evolution of the Magellanic Clouds, IAU Symp. No. 108,* p. 67, eds van den Bergh, S. & de Boer, K. S., Reidel, Dordrecht, Holland.

MacGillivray, H. T. & Stobie, R. S., 1984. *Vistas Astr.,* **27,** 433.

Martin, N., Maurice, E. & Lequeux, J., 1989. *Astr. Astrophys.,* **215,** 219.

Mateo, M., 1988. *Astrophys. J.,* **331,** 261.

Mateo, M. & Hodge, P. W., 1985. *Publs astr. Soc. Pacif.,* **97,** 753.

Mathewson, D. S., Ford, V. L. & Visvanathan, N., 1986. *Astrophys. J.,* **301,** 664.

Mathewson, D. S., Wayte, S. R., Ford, V. L. & Ruan, K., 1987. *Proc. astr. Soc. Aust.,* **7,** 19.

Melcher, N. & Richtler, T., 1989. In: *Recent Developments of Magellanic Cloud Research,* p. 87, eds de Boer, K. S., Spite, F. & Stasinska, G., Observatoire de Paris (GC7).

Mermilliod, J. C., 1981a. *Astr. Astrophys. Suppl.,* **44,** 467.

Mermilliod, J. C., 1981b. *Astr. Astrophys.,* **97,** 235.

Mould, J. R., Da Costa, G. S. & Crawford, M. D., 1984. *Astrophys. J.*, **280,** 595 (GC2).
Murai, T. & Fujimoto, M., 1980. *Publs astr. Soc. Japan,* **32,** 581.
Olszewski, E. W., Schommer, R. A. & Aaronson, M., 1987. *Astr. J.,* **93,** 565 (GC4).
Penny, A. J. & Dickens, R. J., 1986. *Mon. Not. R. astr. Soc.,* **220,** 845.
Rich, R. M., Da Costa, G. S. & Mould, J. R., 1984. *Astrophys. J.,* **286,** 517 (GC3).
Searle, L. & Zinn, R., 1978. *Astrophys. J.,* **225,** 357.
Seidel, E., Demarque, P. & Weinberg, D., 1987. *Astrophys. J. Suppl.,* **63,** 917.
Stryker, L. L., 1984a. *Astrophys. J. Suppl.,* **55,** 127.
Stryker, L. L., 1984b. In: *Structure and Evolution of the Magellanic Clouds, IAU Symp. No. 108,* p. 79, eds van den Bergh, S. & de Boer, K. S., Reidel, Dordrecht, Holland.
Stryker, L. L. & Butcher, H. R., 1981. In: *Astrophysical Parameters for Globular Clusters, IAU Colloq. No. 68,* p. 255, eds Philip, A. G. D. & Haynes, D. S., L. Davis Press, New York.
Stryker, L. L., Da Costa, G. S. & Mould, J. R., 1985. *Astrophys. J.,* **298,** 544 (GC5).
Stryker, L. L., Nemec, J. M., Hesser, J. E. & McClure, R. D., 1984. In: *Structure and Evolution of the Magellanic Clouds, IAU Symp. No. 108,* p. 43, eds van den Bergh, S. & de Boer, K. S., Reidel, Dordrecht, Holland.
Suntzeff, N. B., Friel, E., Kremola, A., Kraft, R. P. & Graham, J. A., 1986. *Astr. J.,* **91,** 275.
VandenBerg, D. A., 1985. *Astrophys. J. Suppl.,* **58,** 711.
van den Bergh, S., 1991. In: *The Magellanic Clouds, IAU Symp. No. 148,* p. 161, eds Haynes, R. & Milne, D., Kluwer, Dordrecht, Holland.
Welch, D. L., McLaren, R. A., Madore, B. F. & McAlary, C. W., 1987. *Astrophys. J.,* **321,** 162.
Westerlund, B. E., 1970. *Vistas Astr.,* **12,** 335.
Westerlund, B. E., 1989. In: *Recent Developments of Magellanic Cloud Research,* p. 159, eds de Boer, K. S., Spite, F. & Stasinska, G., Observatoire de Paris.
Westerlund, B. E., 1990. *Astr. Astrophys. Rev.,* **2,** 29.
Westerlund, B. E., 1991. In: *The Magellanic Clouds, IAU Symp. No. 148,* p. 15, eds Haynes, R. & Milne, D., Kluwer, Dordrecht, Holland.

APPENDIX A

This appendix presents CCD sequences used for calibration of photographic photometry in ESO/SERC Fields 30 and 29. One set of bright and faint sequences lay in the area overlapping the two fields and was used for calibrating both fields.

Appendix A – *continued*

ID no.	RA (1950)	DEC (1950)	*B*	*R*
F30				
1001	02 06 04	-74 58 28	15.91	16.19
1002	02 06 11	-74 59 23	17.84	18.05
1003	02 06 20	-75 01 41	18.43	18.61
1004	02 06 27	-74 58 32	18.44	17.74
1005	02 06 18	-75 00 02	18.50	18.74
1006	02 06 16	-75 00 40	18.65	18.90
1007	02 06 29	-74 59 09	19.36	19.53
1008	02 06 12	-74 59 35	19.41	19.32
1009	02 06 02	-75 00 49	19.78	–
1010	02 06 16	-75 01 08	19.97	19.94
1011	02 06 27	-75 00 04	20.03	19.34
1012	02 06 13	-74 58 12	–	17.40
1013	02 06 15	-74 59 44	–	17.80
1014	02 06 16	-74 59 33	–	18.87
F30 cont.				
2001	02 09 43	-75 07 54	11.84	11.06
2002	02 09 54	-75 08 51	13.49	12.54
2003	02 09 36	-75 10 07	16.58	15.63
2004	02 09 34	-75 09 40	–	10.74
3001	02 39 06	-76 18 04	16.71	15.09
3002	02 38 56	-76 19 27	17.05	15.86
3003	02 38 55	-76 20 26	17.38	15.07
3004	02 38 49	-76 18 06	17.59	16.57
3005	02 39 23	-76 19 07	17.73	16.57
3006	02 38 45	-76 20 37	18.07	16.98
3007	02 38 52	-76 18 40	18.68	17.57
3008	02 39 08	-76 18 20	19.76	18.67
3009	02 39 01	-76 20 29	19.99	19.13
3010	02 39 05	-76 20 12	20.90	18.34
3011	02 39 00	-76 19 50	21.25	–
3012	02 39 02	-76 20 00	21.38	19.58
3013	02 39 23	-76 18 30	–	19.62
4001	02 40 45	-76 23 30	12.31	11.64
4002	02 41 06	-76 24 17	13.62	11.95
4003	02 41 09	-76 23 16	17.06	15.58
5001	02 36 06	-73 18 37	16.41	15.27
5002	02 36 03	-73 19 32	17.25	16.14
5003	02 36 34	-73 19 13	18.00	17.29
5004	02 36 04	-73 21 19	18.53	18.67
5005	02 36 08	-73 19 15	19.45	18.16
5006	02 36 23	-73 19 35	19.51	18.94
5007	02 36 18	-73 19 00	20.19	17.52
5008	02 36 23	-73 20 07	20.34	18.87
5009	02 36 21	-73 19 28	20.85	19.41
5010	02 36 06	-73 20 09	21.03	–
5011	02 36 05	-73 17 53	21.21	18.90
5012	02 36 17	-73 19 56	–	16.22
5013	02 36 18	-73 20 09	–	18.46
5014	02 36 19	-73 20 01	–	19.07
5015	02 36 25	-73 20 58	–	19.34
5016	02 36 19	-73 17 50	–	20.24
6001	02 36 10	-73 11 58	12.64	11.61
6002	02 36 20	-73 14 26	12.72	11.86
6003	02 36 10	-73 13 37	13.33	12.51
6004	02 36 19	-73 11 39	15.12	13.55
6005	02 35 59	-73 11 14	16.08	14.01
6006	02 36 02	-73 13 58	17.22	16.19
F30/29				
7001	01 35 25	-76 20 43	15.65	14.53
7002	01 35 34	-76 23 02	15.70	14.52
7003	01 35 21	-76 22 12	15.90	15.09
7004	01 35 26	-76 22 27	16.61	13.98
7005	01 35 44	-76 21 53	17.39	16.24
7006	01 35 36	-76 19 38	17.67	16.81
7007	01 35 29	-76 19 53	18.01	15.76
7008	01 35 17	-76 20 04	18.92	17.09
7009	01 35 20	-76 19 59	18.97	17.25
7010	01 35 42	-76 19 49	19.11	17.55
7011	01 35 42	-76 21 24	19.69	–
7012	01 35 21	-76 21 15	19.83	18.85
7013	01 35 41	-76 21 37	20.09	19.00
7014	01 35 12	-76 20 25	20.15	19.14
7015	01 35 38	-76 19 57	20.24	17.84
7016	01 35 50	-76 21 22	20.27	18.86
7017	01 35 46	-76 21 41	20.40	18.99
7018	01 35 46	-76 22 08	20.49	19.02
7019	01 35 26	-76 20 30	20.56	–
7020	01 35 12	-76 20 49	20.69	–
7021	01 35 29	-76 20 08	21.00	–
7022	01 35 16	-76 22 43	21.10	18.50
7023	01 35 30	-76 21 51	21.21	–
7024	01 35 33	-76 21 14	–	19.36
7025	01 35 29	-76 22 56	–	19.34

Appendix A – *continued*

ID no.	RA (1950)	DEC (1950)	*B*	*R*
F30/29 cont.				
8001	01 38 06	-76 06 32	13.08	12.18
8002	01 38 34	-76 08 23	15.99	14.59
8003	01 38 16	-76 06 38	16.37	14.43
8004	01 38 40	-76 06 56	–	17.32
8005	01 38 09	-76 09 47	–	18.25
F29				
9001	01 14 36	-74 51 02	17.68	15.82
9002	01 14 45	-74 51 03	18.31	15.86
9003	01 14 50	-74 51 31	18.86	18.15
9004	01 14 57	-74 52 09	18.93	17.77
9005	01 14 44	-74 49 23	19.16	19.19
9006	01 14 43	-74 51 56	19.55	17.92
9007	01 14 43	-74 51 06	19.74	18.25
9008	01 14 51	-74 51 02	19.76	18.53
9009	01 14 56	-74 51 58	19.84	–
9010	01 14 55	-74 51 33	19.97	18.57
9011	01 14 30	-74 52 05	20.06	18.76
9012	01 14 34	-74 50 41	20.09	18.71
9013	01 14 40	-74 53 11	20.29	18.92
9014	01 14 53	-74 51 58	20.31	19.15
9015	01 14 27	-74 52 20	20.33	19.01
9016	01 14 26	-74 50 40	20.33	–
9017	01 14 53	-74 49 29	20.46	19.20
9018	01 14 44	-74 51 34	20.62	19.15
9019	01 14 47	-74 49 29	20.88	–
9020	01 14 35	-74 52 05	21.05	–
9021	01 14 43	-74 51 19	21.16	–
9022	01 14 50	-74 52 00	21.18	19.92
9023	01 14 38	-74 52 39	21.22	18.78
9024	01 14 48	-74 51 19	21.26	19.33
9025	01 14 52	-74 52 15	21.28	–
9026	01 14 57	-74 51 41	21.28	–
9027	01 14 37	-74 52 26	21.28	–

Appendix A – *continued*

ID no.	RA (1950)	DEC (1950)	*B*	*R*
F29 cont.				
9028	01 14 47	-74 50 11	21.41	–
9029	01 14 27	-74 51 05	21.46	–
9030	01 14 26	-74 51 51	21.50	–
9031	01 14 55	-74 51 11	21.52	–
9032	01 14 56	-74 50 54	21.56	–
9033	01 14 26	-74 53 05	21.56	–
9034	01 14 59	-74 50 41	21.60	–
9035	01 14 41	-74 51 10	21.61	–
9036	01 14 26	-74 51 14	21.62	–
9037	01 14 35	-74 49 35	21.62	–
9038	01 14 33	-74 50 27	21.65	–
9039	01 14 48	-74 51 36	21.67	–
9040	01 14 32	-74 52 07	21.67	–
9041	01 14 46	-74 52 14	21.74	–
9042	01 14 27	-74 49 37	21.81	–
9043	01 14 25	-74 52 49	21.81	–
9044	01 14 29	-74 49 42	22.06	–
9045	01 14 48	-74 50 48	22.07	–
9046	01 14 36	-74 50 21	22.28	–
9047	01 14 25	-74 50 38	–	16.22
9048	01 14 35	-74 50 45	–	18.79
9049	01 14 57	-74 50 27	–	19.01
9050	01 14 55	-74 53 11	–	19.35
9051	01 14 25	-74 52 07	–	19.80
0001	01 12 31	-74 50 58	13.66	12.52
0002	01 12 25	-74 51 26	15.72	14.81
0003	01 12 28	-74 51 34	17.17	15.99
0004	01 12 26	-74 50 12	18.09	16.33
0005	01 12 29	-74 48 59	–	11.08
0006	01 12 27	-74 49 33	–	12.18
0007	01 12 20	-74 49 50	–	16.83
0008	01 12 46	-74 50 04	–	17.78
0009	01 12 42	-74 48 27	–	18.94

1992MNRAS.257..195G

APPENDIX B

Selected colour–magnitude diagrams of 0°.93 × 0°.93 grid regions from all six survey fields are presented in this appendix. The field number, distance from the optical centre and position angle with respect to the optical centre (increasing NESW) are labelled on each CMD.

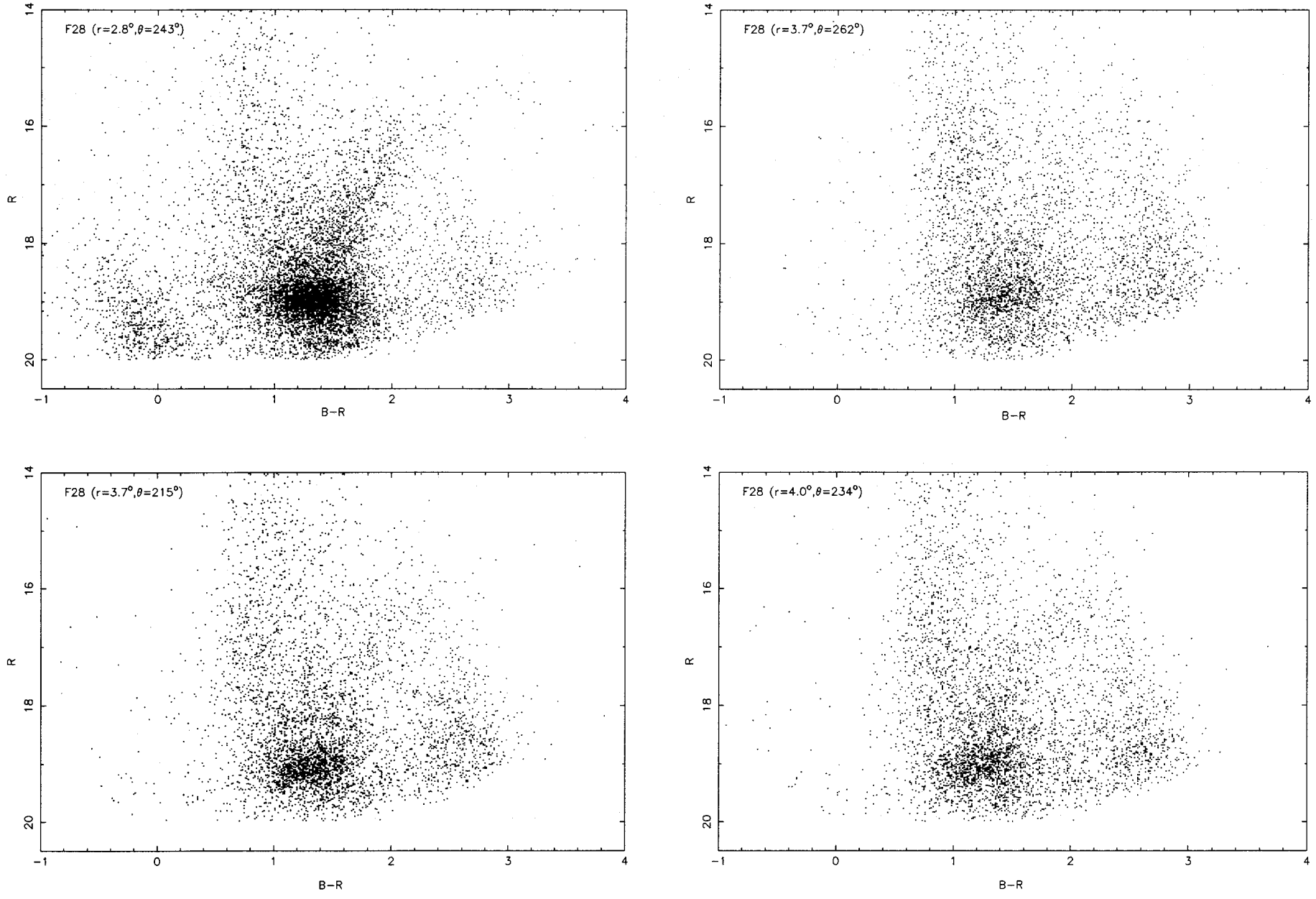

1992MNRAS.257..195G

Appendix B – *continued*

Appendix B – *continued*

1992MNRAS.257..195G

Appendix B – *continued*

Appendix B – *continued*

1992MNRAS.257..195G

1992MNRAS.257..195G

Appendix B – *continued*